



**UNIVERSITY KASDI MERBAH OUARGLA**



**Faculty:** Hydrocarbons and Energy

Renewable and Earth sciences and the universe

**Department:** Renewable Energy

**MEMORY**

**ACADEMIC/PROFESSIONAL MASTER**

**Specialty:** Mechanical Engineering

**Option:** Renewable Energy in mechanics

**Presented by:**

Oussama AOUISSAT

Mohammed Djebbar FACI

Bilal DJEDIRA

**Theme**

*Study of performance and optimization of stand-alone solar dish Stirling system for electricity generation*

Delivered on date:

The: 07/06/2022

In front of the jury:

BOUCHKIMA Bachir

PR

President

UKM Ouargla

DERNOUNI Mohammed

MAA

Framed

UKM Ouargla

NECIB Hichem

MCB

Examiner

UKM Ouargla

**Année universitaire 2021/2022**

# Dedication

## أسامة عويسات

إلى ملاكي في الحياة إلى معنى الحب والى معنى الحنان والتفاني إلى بسمة الحياة وسر الوجود إلى من كان دعائها سر  
نجاحي وحنانها بلسم جراحي إلى أعلى الحبايب أمي الحبيبة.  
إلى النجم الساري في سماء أفقي إلى الغالي الذي سكن في أعماقي إلى منبع الخير الدافق والحنان الوافر... أبي العزيز  
إلى إخوتي وأخواتي كل باسمه دون استثناء إلى أصدقائي وزملائي الأعزاء و أساتذتي الأكارم.

# Dedication

## محمد جبار فاسي

إلى الينبوع الذي لا يمل العطاء إلى من حاكت سعادتي بخيوط منسوجة من قلبها والدتي العزيزة.  
إلى من سعى لأنعم بالراحة والهناء ولم يبخل بشيء من أجل دفعي في طريق النجاح الذي علمني أن أرتقي سلم الحياة  
بحكمة وصبر والدي العزيز.  
إلى من حبهم يجري في عروقي و يلهج بذكراهم فؤادي إلى إخوتي وأخواتي.  
إلى من سرنا ونحن نشق الطريق معا نحو النجاح والإبداع إلى من تكافلنا يدا بيد ونحن نقطف زهرة تعلمنا إلى أصدقائي  
وزملائي.  
إلى من علموني حروفا من ذهب وكلمات من درر وعبارات من أسمى وأجلى عبارات في العلم إلى من صاغوا لي من  
علمهم حروفا ومن فكرهم منارة تنير لنا مسيرة العلم والنجاح إلى أساتذتي الكرام.

والله ولي التوفيق

# Dedication

## جديرة بلال

- ❖ إلى كل من علمني حرفا في هذه الدنيا الفانية.
- ❖ إلى روح أبي الزكية الطاهرة.
- ❖ إلى روح أمي العزيزة الغالية التي سهرت من أجلي.
- ❖ إلى إخوتي وجيراني وأصدقائي الأعزاء.
- ❖ إلى جميع أفراد الأسرة التربوية في الجزائر الحرة الأبية.
- ❖ إلى كل هؤلاء وهؤلاء اهدي هذا العمل المتواضع.
- ❖ ونسأل الله أن يجعله نبراس لكل طالب علم.

Thanks

## Thanks and estimation

- ❖ We thank God Almighty, who with his grace and grace, we were able to accomplish this note.
  
- ❖ We extend our gratitude and thanks to Dr. **Muhammad Darnouni** for his guidance and his remarks and criticism, as well as for his patience throughout the supervision of this note. Despite the multiplicity of obligations.
  
- ❖ We also thank all professors who provided us with assistance, whatever its nature, and to everyone who gave us encouragement, regardless of its degree.
  
- ❖ We also extend our sincere thanks to all our distinguished professors in the renewable energies department for what they provided us during the period of formation, in particular **Omar Rouag**
  
- ❖ We also extend our sincere thanks to the officials of detective 15 **Hamid and Djamel ...**

## Index

Dedication.....	II
Thanks and estimation .....	V
Index.....	VI
List of figures.....	IX
List of tables.....	X
Nomenclature.....	XI
General introduction .....	- 1 -

### Chapter I: Generalities about solar concentrators

1 Introduction:.....	- 4 -
2. General concepts.....	- 4 -
2.1 Basic of solar radiation.....	- 4 -
2.1.1 Diffuse radiation .....	- 4 -
2.1.2 Solar radiation.....	- 6 -
2.1.3 Global solar radiation.....	- 6 -
2.1.4 Energy and Radiation.....	- 7 -
3. Three Concentrating Solar Power (CSP) .....	- 8 -
3.1. Concentrate types:.....	- 9 -
3.1.1. Solar towers .....	- 9 -
3.1.2. Parabolic troughs .....	- 10 -
3.1.3. Linear Fresnel Reflectors.....	- 11 -
3.1.4. Dishes.....	- 11 -
Chapter summary:.....	- 12 -

### Chapter II: A Theoretical study of the stirling system

1. Introduction:.....	- 14 -
2. Introduction to Greenius: .....	- 14 -
3. Introduction System Advisor Model: .....	- 15 -
4. System description:.....	- 16 -
5. Engine Mechanics and Power Cycle: .....	- 18 -
6. Theoretical analysis: .....	- 19 -
.6.1 Energy balance of the dish-Stirling system:.....	- 19 -
6.2. Carnot cycle efficiency of the Stirling engine.....	- 25 -
6.3. Ratio of temperature.....	- 26 -
6.4. The efficiency of the Stirling engine.....	- 27 -
6.5. A linear model of dish-Stirling electric power generation.....	- 28 -
6.6. The net output power generated by the plant and the normal direct radiation hitting the collector mirrors .....	- 29 -

Tables of contents

6.7.	The thermal losses from the receiver .....	- 30 -
<b>Chapter III: Simulation by software GREENIUS</b>		
1	An introduction .....	- 32 -
2	Simulation by software GREENIUS .....	- 32 -
2.1	The Northern States .....	- 32 -
2.1.1	Dish output (E-grid).....	- 32 -
2.1.2	Analysis and discussion .....	- 33 -
2.2	Irradiation on dish area (H-sol).....	- 33 -
2.2.1	Analysis and discussion .....	- 34 -
2.3	Interpretation.....	- 36 -
3	The eastern states .....	- 37 -
3.1	Dish output.....	- 37 -
3.1.1	Analysis and discussion .....	- 38 -
3.2.	rradiation on dish area (H-sol) .....	- 38 -
3.2.1	Analysis and discussion .....	- 39 -
3.3	Interpretation.....	- 42 -
4	The southern states.....	- 42 -
4.1	Dish output (E-grid).....	- 42 -
4.1.1	Analysis and discussion .....	- 43 -
4.2	Irradiation on dish area (H-sol).....	- 43 -
4.2.1	Analysis and discussion .....	- 44 -
4.3	Interpretation.....	- 46 -
5	The western states .....	- 47 -
5.1	Dish output (E-grid) .....	- 47 -
5.1.1	Analysis and discussion .....	- 48 -
5.2	Irradiation on dish area (H-sol).....	- 48 -
5.2.1	Analysis and discussion .....	- 49 -
5.3	Interpretation.....	- 52 -
6	Summary of the third chapter .....	- 52 -
<b>Chapter IV: simulation by system advisor model SAM and An applied simulation</b>		
1.	An introduction .....	- 54 -
2.	Simulation by software SAM .....	- 54 -
2.1	The northern states .....	- 54 -
2.1.1	Analysis and discussion .....	- 55 -
2.1.2	Interpretation.....	- 55 -
2.2	The eastern states .....	- 55 -
2.2.1	Analysis and discussion .....	- 57 -

## Tables of contents

2.2.2 Interpretation.....	- 57 -
2.3 The southern states of Algeria.....	- 57 -
2.3.1 Analysis and discussion .....	- 58 -
2.3.2 Interpretation.....	- 58 -
2.4 The western states of Algeria .....	- 58 -
2.4.1 Analysis and discussion .....	- 60 -
2.4.2 Interpretation.....	- 60 -
3. An applied simulation.....	- 60 -
3.1 Analysis and interpretation .....	- 65 -
4. ideal stirling cycle calculator.....	- 66 -
4.1 calculator inputs.....	- 66 -
4.2 calculator outputs.....	- 67 -
4.3 analysis and discussion.....	- 68 -
5. Summary of the Forth .....	- 69-
<b>General conclusion</b>	
General Conclusion.....	- 70 -
Bibliographic References.....	- 73 -



## List of figures

### Chapter I: generalities about solar concentrators

Fig.I.1.	Composition of the solar radiation reaching the terrestrial surface ArcGIS [2010]	5
Fig.I.2.	Mie and Rayleigh scattering Willis[2010]	5
Fig.I.3.	Shorts wave and long-wave radiation spectrum Illinois central college	6
Fig.I.4.	Sun and earth irradiation	7
Fig.I.5.	CSP technologies	8
Fig.I.6.	Main typical CSP technologies: a) parabolic trough; b) Fresnel reflector; c) solar tower; d) dish/stirling	9
Fig.I.7.	Solar tower power with heliostats	10
Fig.I.8.	Parabolic troughs	11
Fig.I.9.	Linear Fresnel reflector	11
Fig.I.10.	Solar dish. The latter (dish/stirling) subject of our study	12

### Chapter II: A theoretical study of the Stirling system

Fig.II.1.	Schematic diagram of the dish system	17
Fig.II.2.	Solar dish Stirling system energetic chain	18
Fig.II.3.	Theoretic Stirling Eric and Otto cycle	19
Fig.II.4.	Stirling engine pistons arranged in the Siemens arrangement	19
Fig.II.5.	Schematic diagram showing the energy balance of the solar collector	21
Fig.II.6.	Schematic diagram showing the energy balance of the PCO	24

### Chapter III: simulation by software GREENIUS

Fig.III.1	dish output of the northern states	34
Fig.III.2	irradiation on dish area of the northern states	35
Fig.III.3	dish output of the eastern states	39
Fig.III.4	irradiation on dish area of the eastern states	40
Fig.III.5	dish output of the southern states	44
Fig.III.6	irradiation on dish area of the southern states	45
Fig.III.7	dish output of the western states	49
Fig.III.8	irradiation on dish area of the western states	50

### Chapter IV: simulation by system advisor model and an applied simulation

## List des figures

Fig.IV.1	Monthly energy of the northern states of Algeria	56
Fig.IV.2	Monthly energy of the eastern states of Algeria	57
Fig.IV.3	Monthly energy of the southern states of Algeria	59
Fig.IV.4	Monthly energy of the western states of Algeria	60
Fig.IV.5	Mini solar dish project	62
Fig.IV.6	Thermometer solar model OMEGA RDXL4SD	63
Fig.IV.7	Thermal pickup	63
Fig.IV.8	Mini anemometers model UT363	63
Fig.IV.9	Solar power Meter	63
Fig.IV.10	temperature in terms of time	64
Fig.IV.11	irradiation in terms of time	65
Fig.IV.12	wind speed in terms of time	66
Fig.IV.13	P-V diagram of the ideal Stirling cycle	68
Fig.IV.14	Carnot and Stirling efficiency diagram	68

# List of tables

## **Chapter III: simulation by software GREENIUS**

III.1	dish output of the northern states	33
III.2	irradiation on dish area of the northern states	35
III.3	technical key results of the northern states of Algeria	36
III.4	Economic key results of the northern states of Algeria	37
III.5	dish output of the eastern states of Algeria	38
III.6	irradiation in dish area of the eastern states of Algeria	40
III.7	technical key results of the eastern states of Algeria	41
III.8	economic key results of the eastern states of Algeria	42
III.9	dish output of the southern states of Algeria	43
III.10	irradiation on dish area of the southern states of Algeria	45
III.11	technical key results of the southern states of Algeria	46
III.12	economic key results of the southern states of Algeria	47
III.13	dish output of the western states of Algeria	48
III.14	irradiation on dish area of the western states of Algeria	50
III.15	technical key results of the western states of Algeria	51
III.16	economic key results of the western states of Algeria	52

## **Chapter IV: simulation by software system advisor model and an applied simulation**

IV.1	monthly energy of the northern states of Algeria	55
IV.2	monthly energy of the eastern states of Algeria	57
IV.3	monthly energy of the southern states of Algeria	58
IV.4	monthly energy of the western states of Algeria	60
IV.5	An applied simulation	64
IV.6	temperature in terms of time	64
IV.7	irradiation in terms of time	65
IV.8	wind speed in terms of time	65
IV.9	calculator input related to the Stirling engine	67
IV.10	calculator output related to the Stirling engine	67

# Nomenclature

$A_a$  : Total collector aperture area [ $m^2$ ].

$A_n$  : Effective reflective surface of the collector (projected mirror area) [ $m^2$ ].

$A_r$  : Receiver equivalent surface area [ $m^2$ ].

$a_1$  : slope of the linear relation between  $\dot{W}_s$  and  $\dot{Q}_{s,in}$  (dimensionless).

$a_2$  : intercept of the linear the relationship between  $\dot{W}_s$  and  $\dot{Q}_{s,in}$  [W].

$b_1$  : slope of the linear relationship between  $\dot{E}_n$  and  $I_b$  [ $Kw \cdot m^2 / W$ ].

$b_2$  : intercept of the linear relationship between  $\dot{E}_n$  and  $I_b$  [W].

$C_g$  : Geometric concentration ratio of the collector (dimensionless).

$\dot{E}_g$  : Gross electric output power [W].

$\dot{E}_n$  : Net electric output power [W].

$\dot{E}_p$  : Total parasitic absorption power [W].

$\dot{E}_p^{ave}$  : Average value of the total parasitic absorption power [W].

$\dot{E}_{p,d}$  : Parasitic absorption power of the dry-cooler and circulation pumps [W].

$\dot{E}_{p,t}$  : Parasitic absorption power of the tracking system [W].

$h_r$  : Natural convective coefficient at receiver surface [ $W / (m^2 \cdot K)$ ].

$I_b$  : Solar beam radiation [ $W / m^2$ ].

$I_b^{max}$  : Maximum design value of the solar beam radiation [ $W/m^2$ ].

$\dot{Q}_{con}$  : Rate of thermal convective losses from the receiver [W].

$\dot{Q}_{rad}$  : Flux of radiant energy emitted from the receiver [W].

$\dot{Q}_{r,in}$  : Thermal energy power absorbed by the receiver [W].

$\dot{Q}_{r,out}$  : Thermal losses from the receiver [W].

$\dot{Q}_{r,out}^{ave}$  : Average value of the thermal losses from the receiver [W].

$\dot{Q}_{sun}$  : Rate of solar energy incident on the mirrors of the collector [W].

$\dot{Q}_{S,in}$  : Thermal power delivered to the Stirling engine [W].

$\dot{Q}_{S,in}^{max}$  : Maximum design value of the thermal power delivered to the Stirling engine [W].

$\dot{Q}_{S,out}$  : Thermal power rejected from the Stirling engine [W].

$R_T$  : Ratio of temperature  $T_0$  to temperature  $T_{air}$  (dimensionless).

$R_T^{ave}$  : Average value of the ratio of temperature  $T_0$  to temperature  $T_{air}$  (dimensionless).

$\dot{W}_S$  : Rate of mechanical work of the Stirling engine [W].

$T_{air}$  : Air temperature [K].

$T_0$  : Reference temperature [K].

$T_c$  : Rejection temperature of the engine working fluid [K].

$T_r$  : Temperature of the receiver surface [K].

$T_h$  : Heat input temperature of the engine working fluid [K].

$T_{sky}$  : Effective sky temperature [K]

$\eta_c$  : Thermal efficiency of the solar collector (dimensionless).

$\eta_e$  : Average electric generator efficiency (dimensionless).

$\eta_{cle}$  : Cleanliness index of the collector mirror (dimensionless).

$\eta_m$  : Factor accounting for the losses of reflective mirror area (dimensionless).

$\eta_0$  : Effective optical efficiency (dimensionless).

$\eta_s$  : Efficiency of the Stirling engine (dimensionless).

$\eta_{s,c}$  : Carnot cycle efficiency of the Stirling engine (dimensionless).

$\eta_{s,ex}$  : Exergetic efficiency of the Stirling engine (dimensionless).

$\alpha$  : Effective absorptivity of the receiver (dimensionless).

$\varepsilon$  : Effective emissivity factor of the receiver (dimensionless).

$\rho$  : Clean mirror reflectance (dimensionless).

$\gamma$  : intercept factor of the solar collector (dimensionless).

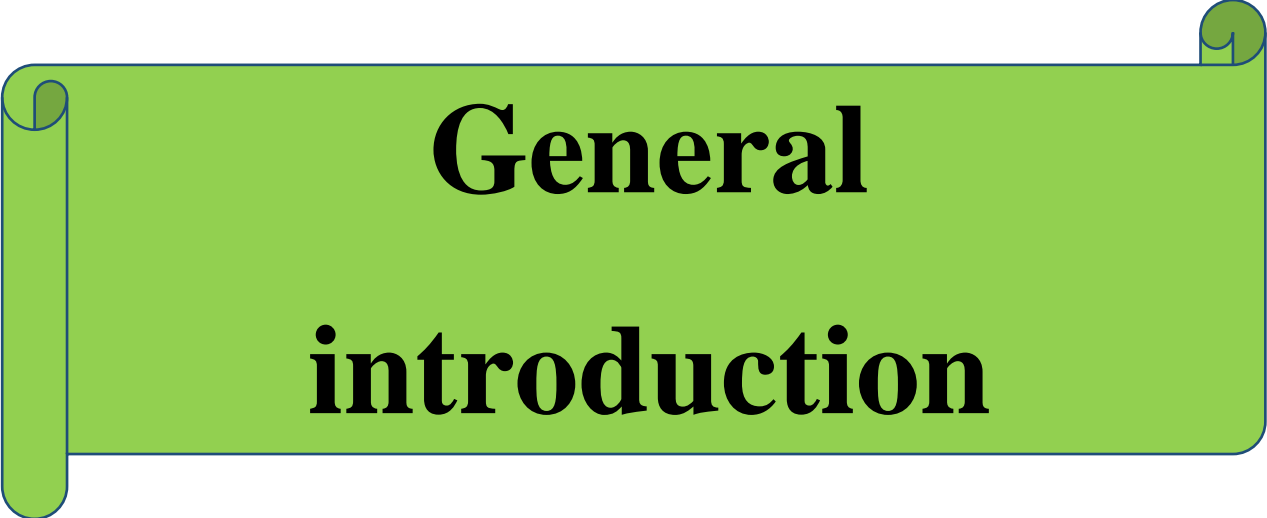
$\sigma$  : Stefan–Boltzmann constant,  $5.67 \times 10^{-8}$  [W/ ( $m^2 \cdot K^4$ )].

Ave: averaged value

Day: mean daily value

Max: maximum design value

Abbreviation	Meaning in english
CSP	Concentrating Solar Power
DP	Parabolic Dish
DNI	Direct Normal Irradiation
GHI	Global Horizontal Irradiance
SEGS	Solar Energy Generating Systems
LCOE	Levelized Costs Of Electricity
IRR	Internal Rate of Return
PCU	Power Conversion Unit
SAM	System Advisor Model
PV	Photovoltaic Panel
DIR	Direct Illumination Receiver
SDK	Software Development Kit
HVAC	Heating, Ventilation, and Air Conditioning
SES	Stirling Energy Systems
IPCC	The Intergovernmental Panel on Climate Change



**General  
introduction**



# General introduction

Interest in generation energy from renewable resources is still growing to meet the large energy demand in near future and protect environment. Solar energy is considered the most attractive renewable energy sources due to their high availability in most regions. Solar powered Stirling engine generators are considered the most efficient system in converting solar energy among all other solar power systems. The net solar -to- electric energy conversion efficiency of Stirling dish system reached 29.4 % in 1984. It is worth mentioning that the efficiency is defined as the net electrical power delivered subtracting the electrical power needed for parasitic, divided by the direct normal irradiation (DNI) incident on the area of the mirrors. Furthermore, in 1984, two 17m -diameter Stirling dish systems (capacity for each =50kWe).were installed and operated in Riyadh in Saudi Arabia. The systems have achieved a net electrical output of 53kW and with net conversion efficiency of 23% at an insolation of 1000 W/m<sup>2</sup>. Recently, large dish/ Stirling plant is constructed in Arizona, United States consists of 60 dishes with a capacity of 25.0kWe each providing a total capacity of 1.5MWe.

Solar Dish Stirling engines have great potential in countries with huge amount of solar radiation. Furthermore, Stirling dish systems are anticipated to outperform parabolic troughs by producing power at more economical rates and higher efficiencies. However, Stirling dish systems have not received significant attention as other solar technologies. They are suitable for hybrid operation due to their ability to combine different heat sources in one application. Due to the fact that parabolic dish concentrates only the direct radiation, two-axes tracking are required to continuously orient the dish towards the Sun. High receiver temperatures obtained from operating high concentration ratios allows highly efficient solar to electric conversion system. However, solar-to-electric efficiency for practical systems is found to range between 16% and 30%.

Stand- alone dish Stirling engine can be used for electricity generation. Research has focused on system reliability, performance, and cost. Finite time thermodynamic and traditional equilibrium thermodynamics are the two main methods for analyzing dish - Stirling engine. Results obtained from finite time thermodynamic method have more realistic instructive significance for the optimal design of real solar-driven systems than those derived from traditional thermodynamic. The optimal efficiency of high temperature differential dish-Stirling engine can reach 34%. High temperature Stirling engine require careful expensive

material selection and high-cost solar collector due to high concentration ratio. Furthermore, due to the seasonal variations of solar radiation, it is not always possible to achieve high receiver temperature. In fact, solar radiation levels change dramatically during the day. The optimal parameters found for high temperature Stirling engine are not necessary optimal for wide range of operating temperature. The objective of this study is to investigate the location-dependent stand-alone dish Stirling engine performance. Parametric study is conducted to investigate the effect of key parameters (receiver aperture diameter, engine heater head operating temperature, and pump operating speed) on system performance. Location dependent parameters include the ambient temperature, density of air (altitude), direct normal insolation, wind speed, and the sun elevation angle [18].

In order to identify the extent to which the solar dish can be exploited and to study the performance and improvement of the Stirling system for generating electricity, we presented a theoretical and experimental study that includes some regions from the north, south, east and west of Algeria. In order to achieve this result, we will discuss in this article.

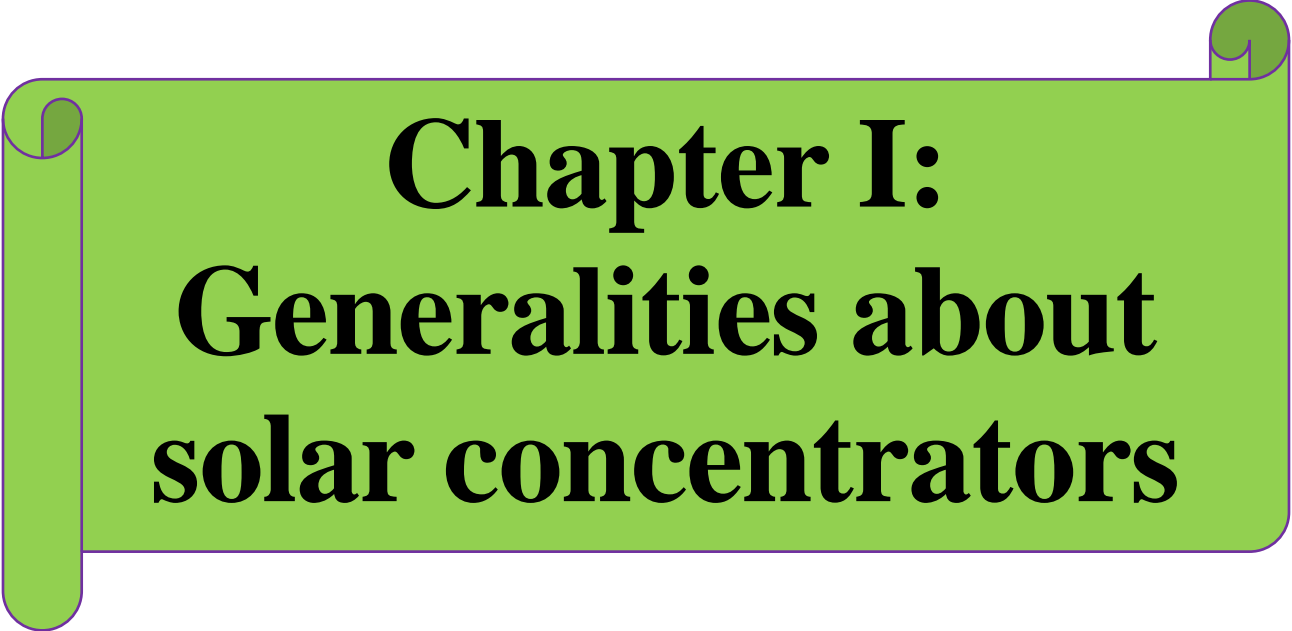
In the first chapter, generalities about solar concentrators, by studying general concepts related to the basics of solar radiation (direct, indirect), solar radiation, as well as the relationship of energy with radiation.

In the second chapter, we will address a theoretical study of the Stirling system, where an overview of the Greenius simulation program and system advisor model is presented, a description of the system and its mechanism of action, through engine mechanics and the energy cycle, and finally the most important relationships and laws related to the solar dish.

In the third chapter, we will study using the simulation program Greenius for some states of the east, west, south and north of Algeria, in order to know the production of the solar dish as well as the radiation of the dish area with a comment on the results.

In the fourth chapter, we will study using the system advisor model simulation program for some as well as the states of the north, south, and east and west of Algeria, then we will turn to the experimental side that contains the stages of completing the experiment, measurements, and used devices.

In the end, we address a conclusion in which we briefly mention everything we discussed in addition to the experimental aspect, and suggest some recommendations and possible solutions in the future.



# **Chapter I: Generalities about solar concentrators**

### **1 Introduction:**

For 30 years, the Intergovernmental Panel on Climate Change (IPCC) has been providing reports proving the climate change and assessing its causes and consequences. In the last report [1], the IPCC highlights the need for the reduction of greenhouse gas emissions in order to control the climate change. The global concern for this issue has led to a strong international support to produce electricity with renewable technologies, such as solar, wind, and biomass, in order to fight the consequences of global warming. Among the renewable technologies, Concentrating Solar Power (CSP) has been acknowledged by the International Energy Agency [1] as an important candidate to produce part of the future electricity needs. However, CSP needs to improve its competitiveness by producing cheaper electricity to assume a more important role in the future electricity market. To decrease the electricity production cost, the technology could reduce construction and maintenance costs, or produce more electricity for the same cost (higher efficiency). Among the multiple ways to achieve these goals, improving the efficiency and durability of a CSP component (keeping costs constant) will directly benefit the competitiveness of CSP. In light of the above, two projects were funded to develop a higher-performance solar receiver for the dish-Stirling CSP technology [2].

### **2. General concepts**

#### **2.1 Basic of solar radiation**

##### **2.1.1 Diffuse radiation**

Can be defined as the short wavelength radiation coming from all parts of the sky [Liu and Jordan, 1960]. It is reflected and scattered and includes multiple reflections between the atmosphere and the surface. Clouds are one of the principal factors responsible for diffuse radiation. There are two main types of scattering (Figure I.2): the Rayleigh scattering and the Mie scattering. The first one is elastic scattering of light by particles, such as atoms and molecules, whose diameter  $d$  is much smaller than the light wavelength  $\lambda$ . Its intensity  $I$  is wavelength dependent ( $I \propto \lambda^{-4}$ ) and is equal for forward and backward scattering. The minimum of its intensity is at  $90^\circ$  of its line of incidence. It explains the blue sky and the red sunsets and sunrises. On the other hand, the Mie scattering is caused by particles, such as dust, pollen and smoke, whose diameter has the same magnitude as the incident light radiation. It often occurs in the lower portion of the atmosphere, where larger particles are

## Chapter I: Generalities about solar concentrators

more abundant, and is mainly in the forward direction. In a clean and dry atmosphere, half of the radiation is scattered back to the space and the other half reaches the surface as diffuse radiation. With more dust in the atmosphere, more scattered radiation reaches the surface because of a forward direction scattering. For this reason, there is a big portion that appears to be from a small annular area around the solar disk: circumsolar radiation. The diffuse radiation generated by the primary scattering is dominant. Ozone absorbs in the ultraviolet, visible and infrared light. The attenuation is very strong in the far-ultraviolet region [Iqbal, 1983]. The amount of radiation reaching the surface without any scattering or reflection is defined as direct radiation. The global radiation is the sum of the two components, diffuse and direct. The diffuse fraction  $K_d$  is affected by the scattering, as it represents the fraction of diffuse radiation compared to the global radiation reaching a location [3].

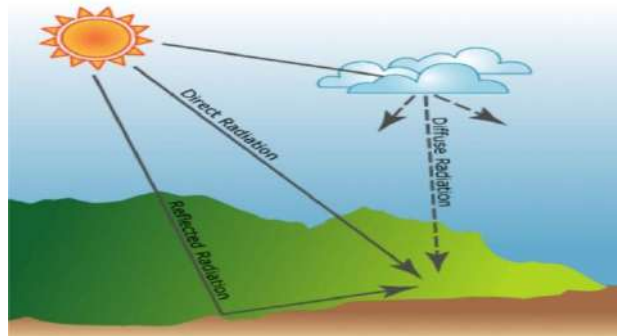


Figure I.1. Composition of the solar radiation reaching the terrestrial surface ArcGIS [2010] [3].



Figure I.2. Mie and Rayleigh scattering Willis [2010] [3].

## Chapter I: Generalities about solar concentrators

### 2.1.2 Solar radiation

Essential energy is provided to the Earth by the Sun in the form of radiation. It is necessary for the life on the Earth. For example, it is the principal constituent of photosynthesis. Radiation describes the process by which the energy is transmitted through the medium by photons. Photons have similar properties as particles and waves. The oscillations can be considered as waves traveling with a wavelength  $\lambda$ . Furthermore, radiation is able to travel in vacuum and moves at the speed of light ( $3 \cdot 10^8$  m/s).

All bodies possessing energy are emitting radiation. For instance, the Sun emits radiation with wavelengths from  $0.15 \mu\text{m}$  (ultra-violet) to  $3.0 \mu\text{m}$  (near infrared) mostly, whereas the Earth-Atmosphere system emits radiations ranging from  $3.0 \mu\text{m}$  to  $100 \mu\text{m}$  (see Figure I.3). For this reason, radiations in the range  $0.15\text{-}3.0 \mu\text{m}$  are designed as short wave or solar radiation, and radiation in the range  $3.0\text{-}100 \mu\text{m}$  are named long-wave radiation [Oke, 1978] [3].

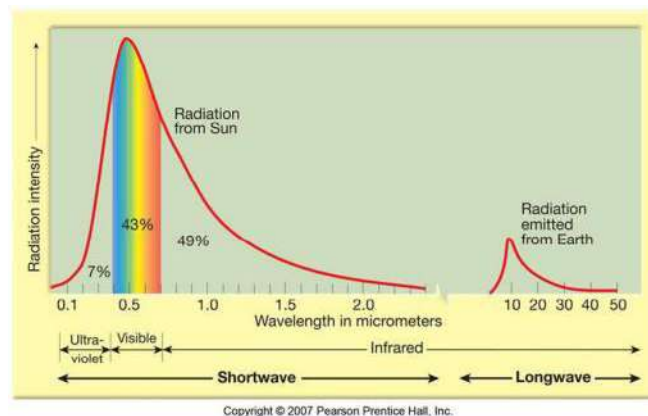


Figure I.3. Short wave and long-wave radiation spectrum Illinois Central College [3].

### 2.1.3 Global solar radiation

Light or electromagnetic radiation that reaches the Earth's surface is partially absorbed on the surface, while the other part is reflected back to the atmosphere. Incoming light, apart from the component that comes directly from the Sun (it means that the light has not encountered obstacles, direction of direct radiation can be determined in each point of Earth's surface), there is also a part of the light that diffusely refracts due to the particles in atmosphere itself (e.g. clouds, dust, smog and other aerosols), in that way it changes the spectral distribution of incident light. Apart from that, the planet Earth itself radiates electromagnetic radiation (Figure I.4). Total radiation that falls on the flat horizontal surface is called global radiation [4].

Global or total radiation consists of three components:

- ✓ Direct,

## Chapter I: Generalities about solar concentrators

- ✓ Diffused or scattered, and
- ✓ Reflected or albedo surfaces.

In many papers, only the first two are mentioned as global radiation components, although sometimes the reflection from surrounding area is significant so it can noticeably change the total light intensity that reaches the plane of solar collector or panel. Due to the revolution and rotation of Earth, only extraterrestrial radiation changes over time, global radiation also changes on horizontal surface so that annual course in radiation occurs. It is the highest at summer and the least at winter, when it is cloudy or foggy, the value is smaller [5].

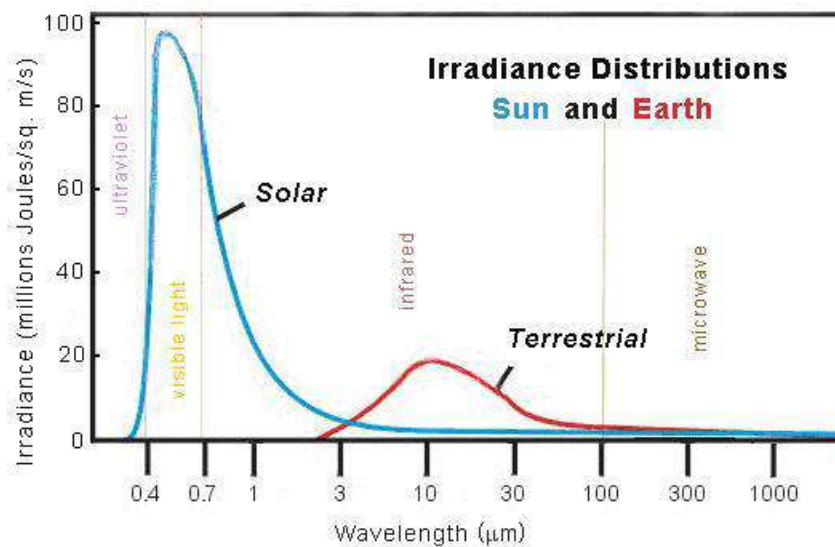


Figure 1.4. Sun and Earth irradiation [4].

### 2.1.4 Energy and Radiation

#### 2.1.4.1 Radiation:

The transfer of energy via electromagnetic waves that travel at the speed of light. The velocity of light in a vacuum is approximately  $3 \times 10^8$  m/s. The time it takes light from the sun to reach the Earth is 8 minutes and 20 seconds. Heat transfer by electromagnetic radiation can travel through empty space. Anybody above the temperature of absolute zero ( $-273.15^\circ\text{C}$ ) radiate energy to their surrounding environment.

The many different types of radiation are defined by its wavelength. The electromagnetic radiation can vary widely [6].

**3. Three Concentrating Solar Power (CSP)**

CSP technology uses a four-stage process to produce electricity. Firstly, mirrors concentrate the solar radiation. Secondly, the concentrated sunlight is converted into high-temperature heat in a solar receiver. Thirdly, the heat is stored either as latent or sensitive heat. This stage is theoretically optional, but necessary in practice since it provides the main advantage of CSP (dispatch ability). Fourthly, a conventional thermal cycle is run to generate electricity. Additionally, CSP can also provide other services for polygene ration technologies, such as cooling, heating, or water purification. Based on the type of mirrors concentrating the sunlight, mainly four CSP technologies are usually considered: central tower, parabolic trough, linear Fresnel and parabolic dish (Fig. I.5). Linear Fresnel and parabolic trough are line-focusing (2D concentration), whereas parabolic dish and central tower are point-focusing (3D). Point-focusing concentration can achieve higher concentration ratios, which increases the system efficiency and operating temperature, but generally, at a higher cost. Nowadays, parabolic trough is considered the most mature CSP technology but point-focusing technologies have higher potential, which still has to be further developed [7].

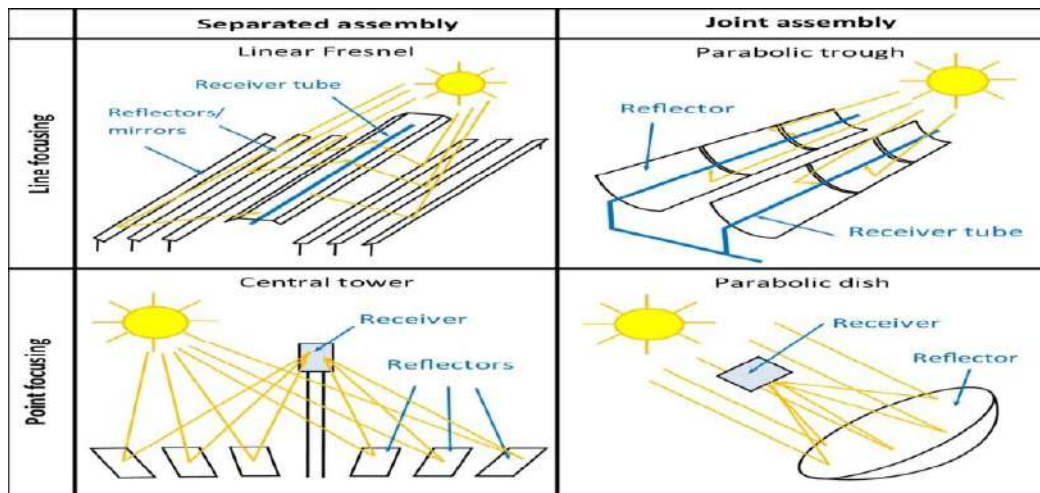


Figure1.5 : CSP technologies [8].



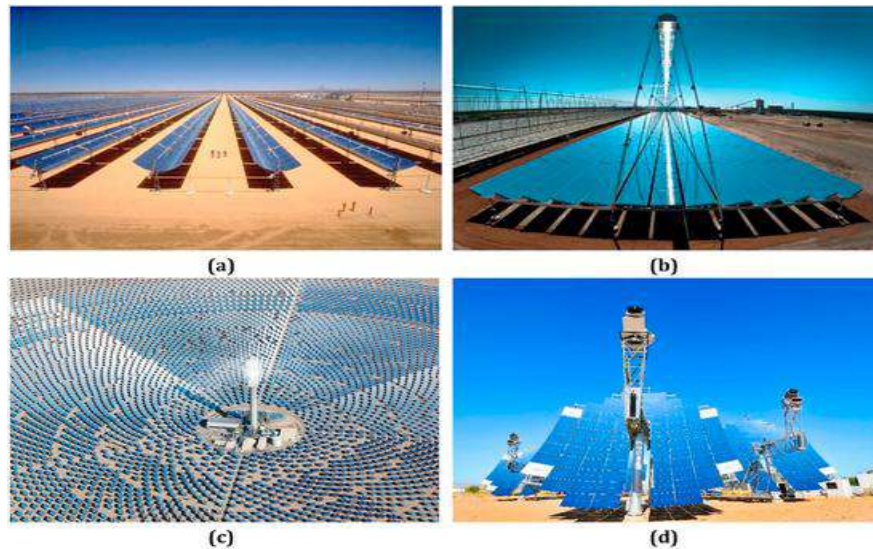


Figure I.6. Main typical CSP technologies: a) Parabolic trough; b) Fresnel reflector; c) Solar tower; and d) Dish/Stirling [9].

### 3.1. Concentrate types:

#### 3.1.1. Solar towers

Solar towers turn the solar energy into electricity by the technology that uses a large number of mirrors tracking the sun called heliostats. A heliostat (from Helios, the Greek word for the sun, and stat, as in stationary) is a device that includes a mirror, usually a plane mirror, which turns to keep reflecting sunlight toward a predetermined target, compensating for the sun's apparent motions in the sky. These heliostats focus the rays of sunlight on the receiver located at the top of the solar tower as can be seen in Figure I.7. The movement of most modern heliostats employs a two-axis motorized system, controlled by a computer. Usually, the primary rotation axis is vertical and the secondary horizontal, so the mirror is on a simple two-axis mount. About half of the cost for the entire installation goes to heliostats and their additional equipment. As mentioned before, the working fluid is heated in the receiver and used to create steam that is used in conventional turbine generators for electricity generation. Earlier constructions of solar towers used steam as a working fluid, while in the present constructions a nitrate salt solution is used to achieve better transmission of heat and storage characteristics. Single commercial systems are able that can produce from 50 to 200 MW of electricity. Some of the largest CSP systems that use solar power towers are Ivanpah Solar Power Facility, with 392 MW of power installed, and Crescent Dunes Solar Energy Project that has 110MW of power installed [10].



Figure I.7. Solar power tower with heliostats [10].

### **3.1.2. Parabolic troughs**

CSP system that uses a trough consists of parabola troughed reflectors (mirrors), which concentrate sunrays into a focal point, which is constructed as an absorber tube. The collector fields contain dozens of parallel rows of tubular collectors arranged along the axis (line) North South as shown in Figure I.8. This configuration allows it to monitor the movement of the sun from east to west during days and provides constant focus on the sun. Tracking of the sun is done by rotating reflectors around the absorber tube. Their position provides a constant reflection of the sun to absorber tube. Heat energy passes through the tube (the working medium is oil) and is used for the production of electricity in a conventional steam generator. Individual trough systems can currently produce about 80 MW of electrical energy. The construction of trunk systems can also contain a thermal warehouse, located next to a heat exchanger at its hot stage (hot part), which allows the generator several hours of operation even after sunset. Currently, parabolic trough systems represent hybrids (mixed systems) [11], which mean that they use combustion of fossil fuels for heating solar output during the reduced period of solar radiation. In addition, trough systems can be integrated with existing thermal power plants. Solar Energy Generating Systems (SEGS) in California, with the combined capacity from three separate locations at 354 megawatts is the second largest CSP facility and it uses parabolic trough with the combustion of natural gas [10].

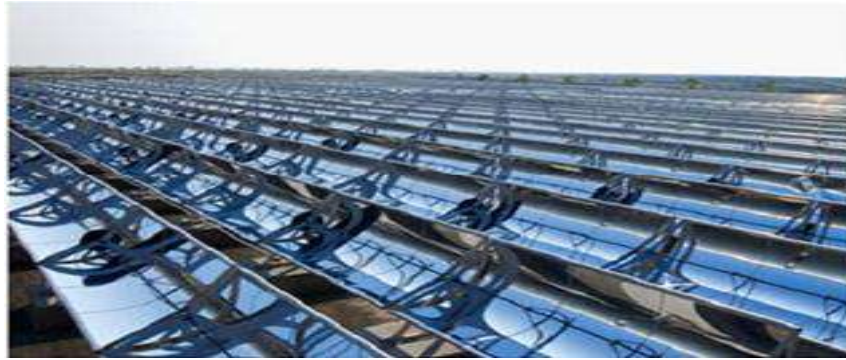


Figure I.8. Parabolic trough [12]

### 3.1.3. Linear Fresnel Reflectors

This type of reflecting mirrors is very frequently considered to belong to the group of solar towers since it has similar construction. Linear Fresnel Reflectors (LFR) use long, thin segments of mirrors to focus sunlight into a fixed absorber located at a common focal point of the reflectors (Figure I.9). These mirrors are capable of concentrating the sun's energy to approximately 30 times its normal intensity. This concentrated energy is transferred through the absorber into a thermal fluid (this is typically oil capable of maintaining a liquid state at very high temperatures). The fluid then goes through a heat exchanger to power a steam generator. Linear Fresnel Reflectors usually employ a secondary concentrator that enlarges the target area for primary mirrors, and acts as a protective cover to reduce convective losses [10].

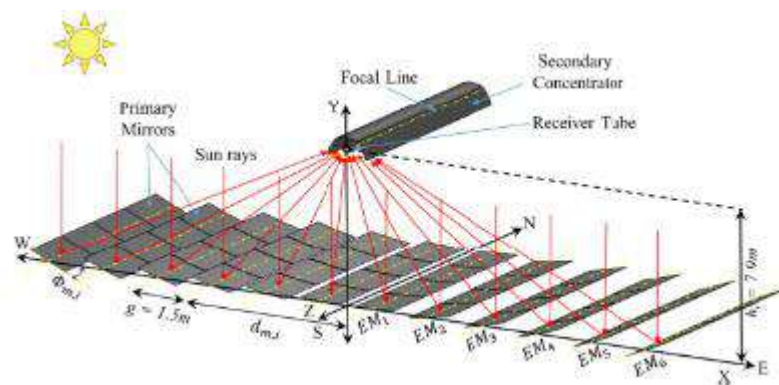


Figure I.9. Linear Fresnel reflector [13]

### 3.1.4. Dishes

Another type of concentrating solar collector that optically reflects and focuses the ray of sunlight onto a small receiving area using mirrors or lenses is called a Solar Dish Collector, or more technically, a point focusing collector (Figure I.10). By concentrating the sunlight to a single spot, the intensity of the receiving solar energy is magnified many times over with each

## Chapter I: Generalities about solar concentrators

mirror or lens acting as a single sun shining directly at the same focal point on the dish meaning that more overall power per square meter of the dish is achieved. Unlike the previous solar collector, which was in the shape of a long trough or has flat mirrors, a parabolic solar dish collector is very similar in appearance to a large satellite TV or radar dish making it much smaller than a long trough collector does. The curved parabolic shaped dish, which is generally referred to as a “solar concentrator” is the main solar component of this type of solar heating system [10].

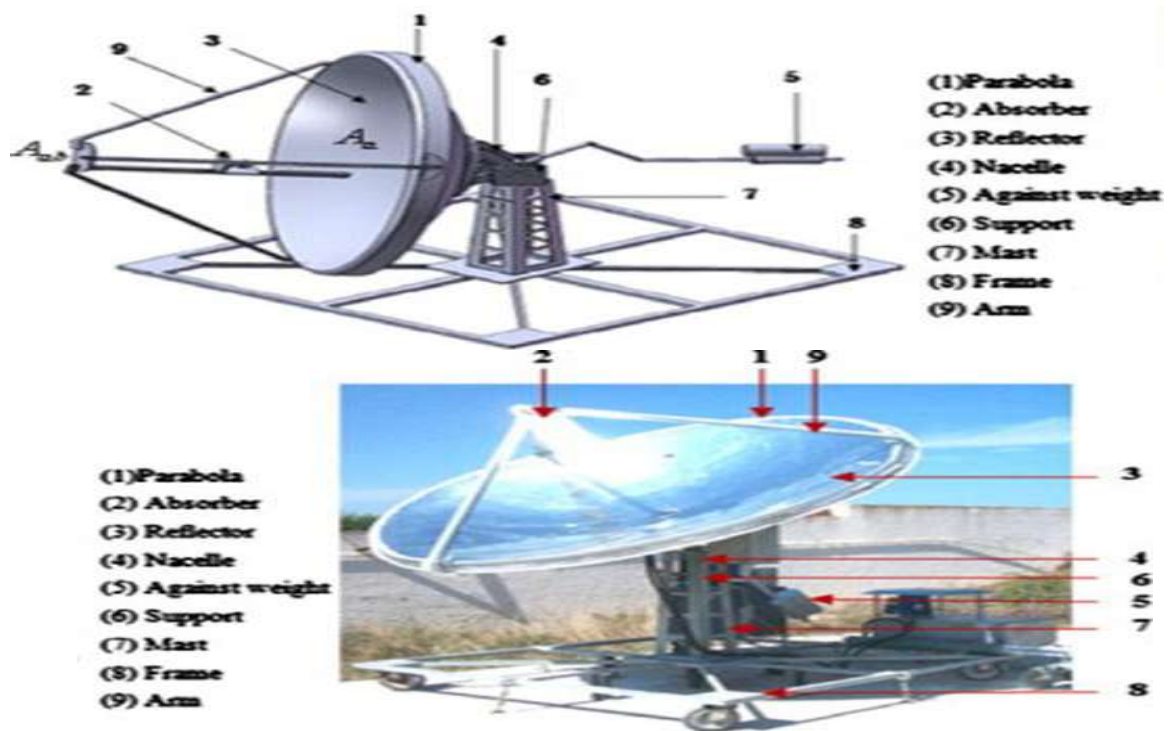
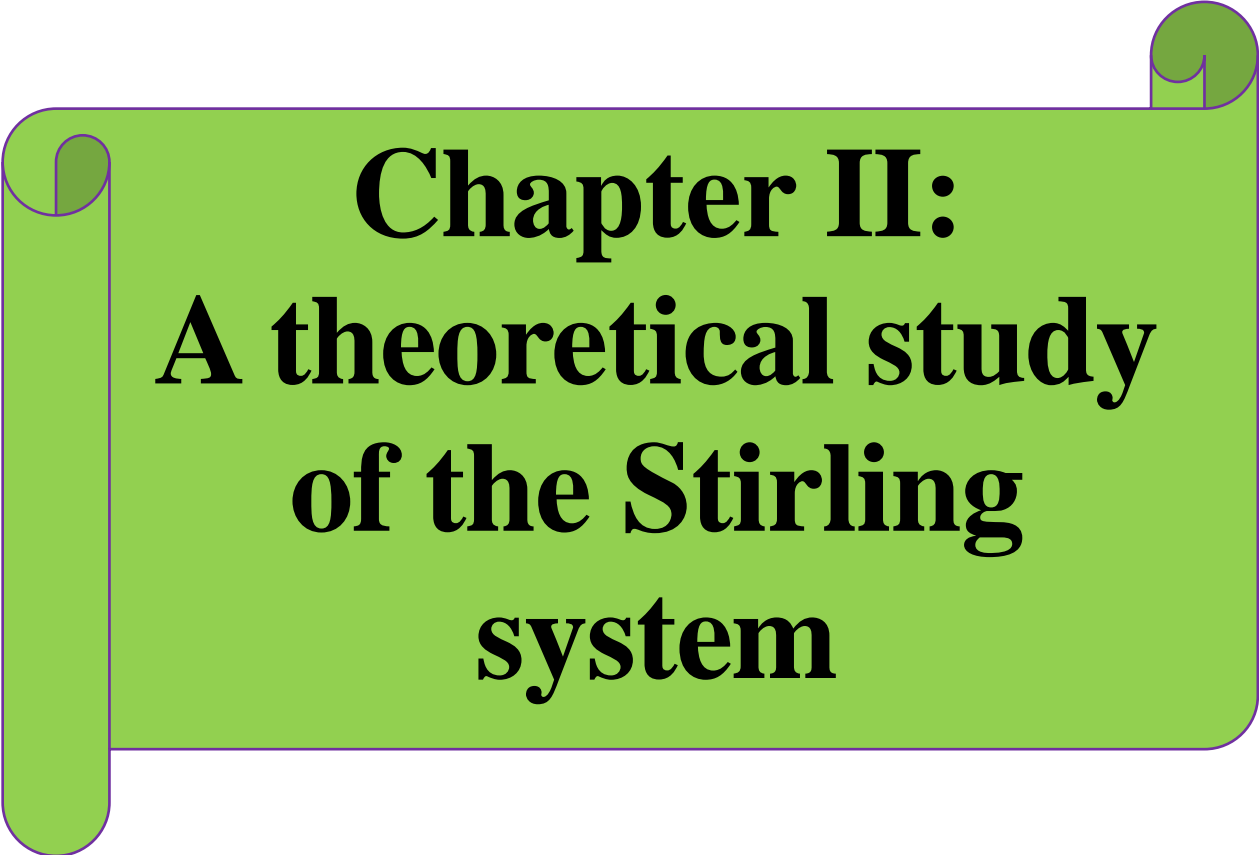


Figure I.10. Solar dish [14]. The latter (Dish/Sterling) subject of our study.

### Chapter summary:

After learning about the basics of solar radiation, the types of solar radiation and the relationship of energy to solar radiation, as well as exposure to different types of solar collectors, we will discuss in the second chapter the study of the theoretically equivalent solar energy dish. By studying some basic concepts and knowing the mechanism of the system's work and the most important mathematical relationships and laws related to the solar dish.



**Chapter II:  
A theoretical study  
of the Stirling  
system**

### **1. Introduction:**

Electric energy is essential to the human activities and to our society, and an increasing demand is expected in the coming years. In this scenario, the use of renewable energy sources for generating electricity is essential for reducing the dependency from fossil fuels and due to environmental concerns. Among the available technologies, Stirling engine systems powered by solar energy are one of the most promising solutions because they combine a readily available resource with a simple and efficient thermal cycle. Stirling engines present several advantages, such as high thermodynamic efficiency, the capability to use any heat source, including fuel, solar, geothermal or waste heat, and low level of noise. These are reasons why it has received the attention of researchers in the last years aiming its modeling, optimization and application in power generation systems. This solution is particularly suitable for small or medium scale solar power plants and its combination with thermal energy storage and the hybridization with other energy sources still are open fields of research to explore [15].

### **2. Introduction to Greenius:**

A specific feature of most renewable energy sources like solar and wind is their fluctuating availability. Thus, the expected total annual production and economic evaluation of power plants generating electricity from solar or wind cannot be estimated just from the calculation of a few steady state operating points. Instead, an annual performance simulation with at least hourly time steps using a typical meteorological year is state-of-the-art. Local conditions like available solar irradiance or wind velocity are the main impact parameters and their instantaneous values determine the plant output. The software tool Greenius is being developed since several years at DLR and since December 2013 a free version with full functionality is available from. It is continuously maintained and developed which includes the addition of new features and bug fixing. Greenius may be used for feasibility studies as well as for technology comparisons, for educational purposes as well as for due diligence studies. Of course Greenius is an engineering tool, not a “one-click-tool”. Users must be careful about the input data as well as capable of evaluating and verifying the output by plausibility checks. However, the given default values and example projects make the access to the software easy. The focus of Greenius is on concentrating solar power plants and for this technology, the most detailed models are implemented. Furthermore, Greenius may simulate the following technologies: process heat generation by concentrating and non-concentrating solar collectors, solar cooling, PV systems and wind power parks. Greenius comes with some

## ***Chapter II: A theoretical study of the stirling system***

---

example projects and users may adapt them to their own needs or create simulation projects from scratch. All input datasets may be edited in order to adapt them to specific conditions prevailing at the individual site. Meteorological data is an input to Greenius and users must provide this dataset in a specific format. Import filters ease the use of several data format typical sources for meteorological data. The default temporal resolution used is one hour but even smaller time steps are possible, down to 10 minutes, if the meteorological data is available in this resolution. Further reduction of time steps is not considered reasonable since it is based on steady state models and cannot be used to study dynamic effects.

Greenius offers also an economical calculation of the renewable power plants considering investment costs, O&M costs as well as financing costs over a user-defined period. Economic output variables are amongst others: Levelized cost of electricity (LCOE), internal rate of return (IRR), and net present value and payback times. It is obvious that the results of the economical calculation will heavily depend on the input for component costs and it should be mentioned that Greenius does not contain an up to date cost database. This task is left to users [16].

### **3. Introduction System Advisor Model:**

The System Advisor Model (SAM) is free software developed by the National Renewable Energy Laboratory that predicts hourly energy production for renewable energy systems. Technologies represented in SAM include photovoltaic (flat-plate and concentrating), concentrating solar power (parabolic troughs, towers, linear Fresnel, dish-Stirling), solar water heating, wind, geothermal, and biomass. Hourly performance models for PV, wind, geothermal, and biomass plants are relatively straightforward computationally, as a series of sub models are executed in sequence to calculate outputs given weather data inputs and system parameters. For concentrating solar thermal models, however, the solution techniques are not so simple. These systems are represented by interconnected individual components such as solar collectors, receivers, heat exchangers, piping, storage systems, and power cycles. Each component cannot be sequentially modeled because pressures, mass flow rates and temperatures at the interfaces between components must match, and energy and mass must be conserved among the piping loops and feedback systems that exist within the system design. Consequently, iterative numerical solutions are applied such that at each time step of the simulation, the system representation has “converged” to physically sensible values at each point. To date, SAM has utilized the general-purpose commercial TRNSYS tool for modeling concentrating solar thermal power plant systems. TRNSYS is a well-established

## ***Chapter II: A theoretical study of the stirling system***

---

software package that has been in development since the mid-1970s and the simulation core and engineering component code is written entirely in FORTRAN and focused at engineers doing desktop system analysis. The software consists of a small kernel that iteratively calls individual system component models many times until the overall system has converged, as well as an extensive library of components such as building models, HVAC systems, geothermal heat pumps, and pipes, tanks with heaters, solar collectors, PV systems, and related equipment. In previous version of SAM dating back to 2007, custom CSP component models have been implemented in FORTRAN in adherence to the TRNSYS conventions. SAM includes only the TRNSYS kernel and component models necessary for CSP modeling at this time. These models have proven to be reliable and capable predictors of system performance and have been validated and utilized in the literature. The motivation to reconsider the use of TRNSYS within SAM has been driven by factors driving the need for simulating very large scenarios that may require thousands of simulations with different input parameters. To achieve these results in a permissible amount of time, it is highly advantageous to effectively utilize modern desktop computer processors that may have up to eight individual cores, as well as provide a software framework that can be deployed on distributing computing systems or dispatched over the internet. There is also a need to support the SAM Software Development Kit (SDK) which does not currently allow users to access CSP technologies through the thermal systems to achieve the aforementioned goals of performance, portability, and parallelism. Preliminary results from the new CSP simulation core software show excellent agreement with the accepted outputs of the TRNSYS versions, as well as significant improvements in simulation speed [17].

### **4. System description:**

The Stirling dish system shown in (Figure II.1) produces electricity using concentrated solar thermal energy to drive a Stirling engine. The main components of system are a) dish collector, b) cavity receiver, c) Stirling engine, d) generator, e) converter, batteries bank, and inverter. The system utilizes a parabolic mirror equipped with dual-axis tracking to concentrate solar radiation onto a thermal receiver integrated in the Stirling engine. The function of the receiver is to transfer the absorbed solar energy to the working fluid in Stirling engine. The Stirling engine converts the absorbed thermal energy into a mechanical power by compressing the working fluid when it is cool and expanding it when it is hot. Through driving mechanism, this linear motion is converted to a rotary motion to turn a generator to produce electricity, as shown in Fig.II.2. The size of the dish typically depends on the needed



## Chapter II: A theoretical study of the stirling system

nominal power of the engine. The concentration of solar radiation is key parameters that affect the engine conversion efficiency.

A Stirling receiver consists of an aperture and an absorber. The aperture in a Stirling receiver is located at the focal point of the parabolic concentrator to reduce radiation and convection losses. The intercept factor usually ranges between 94% and 99%. Direct-illumination receiver (DIR) is considered for Stirling absorbers in this study. Direct-illumination receiver has a bank of tubes to directly heat the working fluid in the Stirling engine using the solar radiation that is absorbed on the external surface of the tubes.

The Stirling cycle is a thermodynamic cycle in which thermal energy is transformed into mechanical energy. Detailed description of Stirling thermodynamic cycle can be found in. A key component of Stirling engines is the regenerator, which stores and releases thermal energy periodically. The existence of regenerator raises the efficiency of the engine by maintaining heat within the system that otherwise would be exchanged with the environment. It reduces the heat flow from the high temperature reservoir to the low temperature reservoir without any additional gain of mechanical work [18].

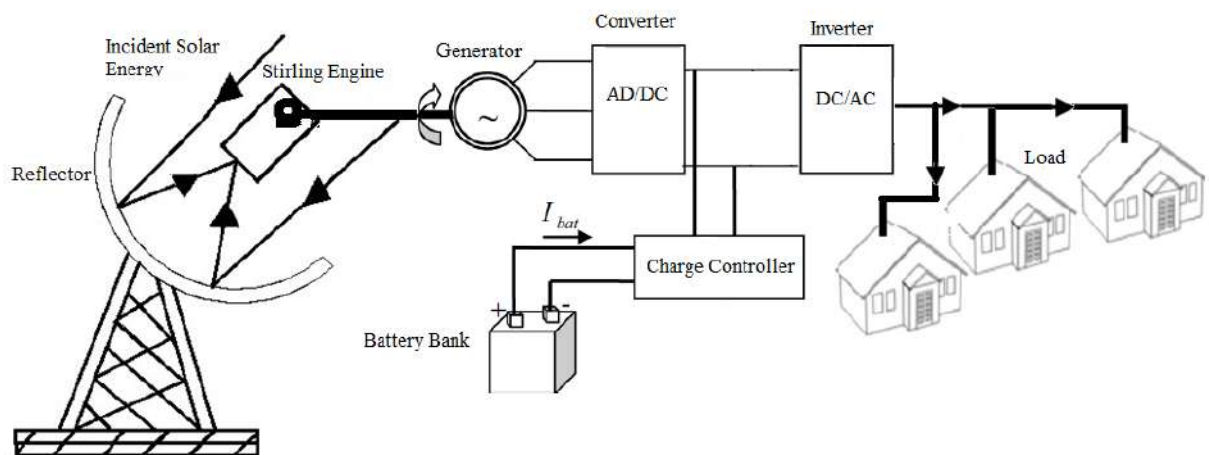


Figure II.1: schematic diagram of the dish system [18].

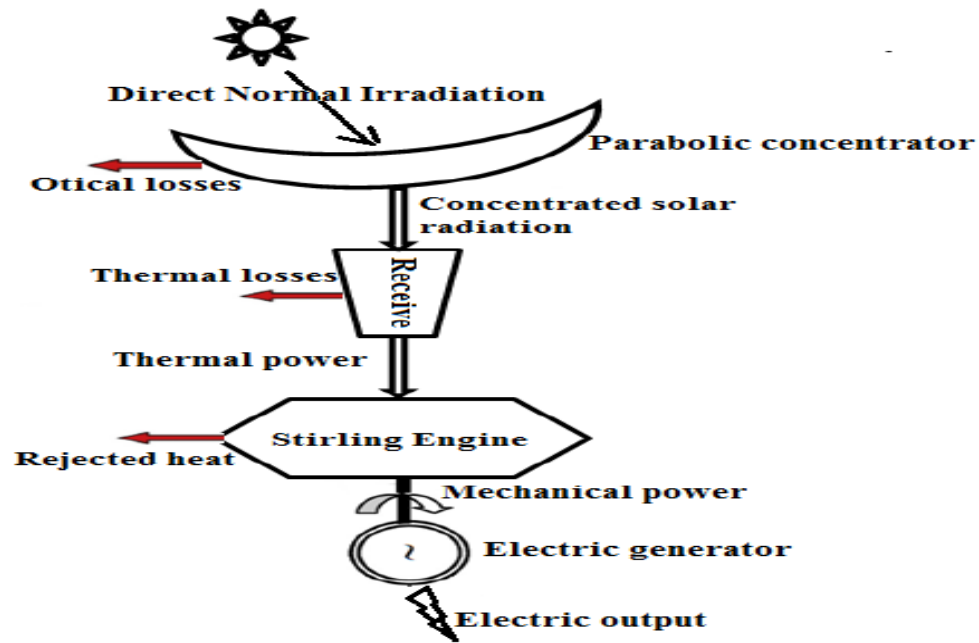


Figure II.2. Solar dish Stirling system energetic chain [18].

### **5. Engine Mechanics and Power Cycle:**

Ideally, the thermodynamic cycle consists of two isothermal and two constant-volume processes: isothermal compression, constant volume heat addition, isothermal expansion and constant volume heat rejection. The actual cycle, with crankshafts and sinusoidal motion of pistons only approaches the thermodynamic efficiency of the ideal cycle. The engine consists of four cylinders, configured similar to figure (II.4) that are connected together in what is called the Siemens arrangement. The hot side of every piston is connected to its neighbors cold side. The larger the pressure difference between the hot and cold side the more powerful the stroke will be. The Stirling engine power cycle is shown in figure (II.3). The gas is heated in the receiver tube, which is connected to the hot side of the piston, the gas expands, and pushing the piston down, this is how torque is generated. The gas is then forced back through the receiver tube where it absorbs more energy. Before the gas enters the cold side of the piston, the gas gives up a large part of its thermal energy to the regenerator. The gas then enters the cold side where it is cooled to maximize the pressure difference between the hot and cold side of the piston. When the piston is pushed down gas is forced back through the regenerator where the stored thermal energy is regained and used in the next stroke. The temperature of the hot-side gas, which is inferred from the highest receiver tube temperatures, is held constant by controlling the amount of hydrogen gas circulating in the system. As the control tube temperature increases due to an increase incident power, gas is added to the cycle

## Chapter II: A theoretical study of the stirling system

from the storage bottle, which increases the coolant flow through the receiver and brings the tube temperature back to the set-point value. When the tube temperature drops due to a reduction in incident power gas is removed from the cycle, compressed, and returned to the high-pressure storage bottle, which reduces coolant flow through the receiver and increases the working gas temperature [19].

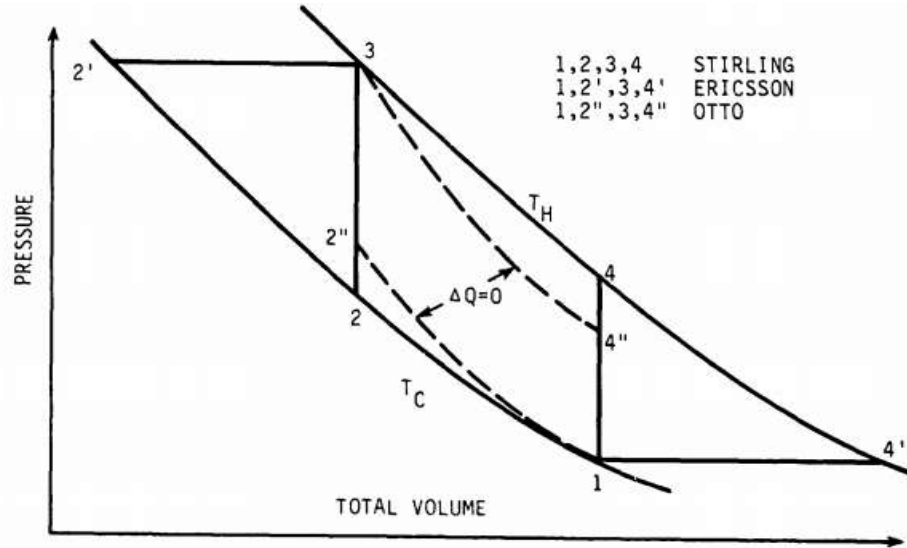


Figure II.3. Theoretic Stirling Eric and Otto cycle [19].

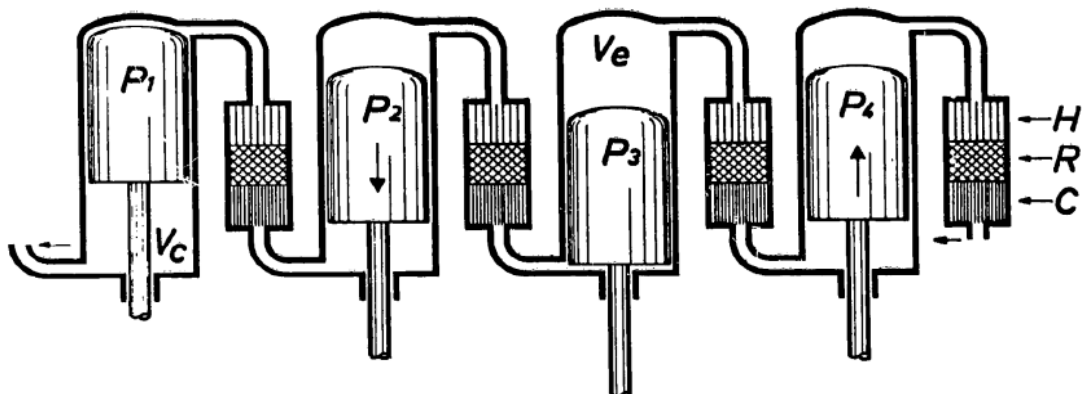


Figure II.4. Stirling engine pistons arranged in the Siemens arrangement [19].

## 6. Theoretical analysis:

### 6.1. Energy balance of the dish-Stirling system:

In dish-Stirling, systems (see Fig.II.5), the mirrors constituting the primary optics of the collector (usually with a parabolic shape) concentrate the sun's light on the focal point of the collector, where a cavity-type receiver absorbs and transfers the concentrated solar energy to a Stirling engine driving an electric generator. Unlike other types of solar collectors

## ***Chapter II: A theoretical study of the stirling system***

---

(photovoltaic and thermal), CSP systems, such as solar dish-Stirling plants, can only transform the direct component of solar radiation into thermal/electric power. Therefore, the rate of solar energy reflected off the mirrors of a collector continuously tracking the sun can be calculated as [20]:

$$\dot{Q}_{sun} = I_b \cdot A_n \quad (\text{II.1})$$

Where:

$\dot{Q}_{sun}$  : Rate of solar energy incident on the mirrors of the collector [W].

$I_b$  : Solar beam radiation [ $\text{W}/\text{m}^2$ ].

$A_n$  : Effective reflective surface of the collector (projected mirror area) [ $\text{m}^2$ ].

The latter quantity can be calculated from the total collector aperture area and by:

$$A_n = \eta_m \cdot A_a \quad (\text{II.2})$$

Where:

$\eta_m$  : Factor accounting for the losses of reflective mirror area (dimensionless).

$A_a$  : Total collector aperture area [ $\text{m}^2$ ].

However, not all of this solar power is effectively reflected off the mirrors, intercepted by the cavity receiver aperture and then absorbed by its surface, because of different factors that affect the optical performances of the collector, the main ones being [20]:

- ❖ reflectance of the mirrors
- ❖ mirror surface slope errors
- ❖ soiling of the mirrors
- ❖ sun tracking system errors
- ❖ receiver positioning errors (often combined with mirror errors)
- ❖ wind-induced vibrations
- ❖ effective absorbance of the cavity receiver
- ❖ water condensation at the mirror surface during the early hours of the day

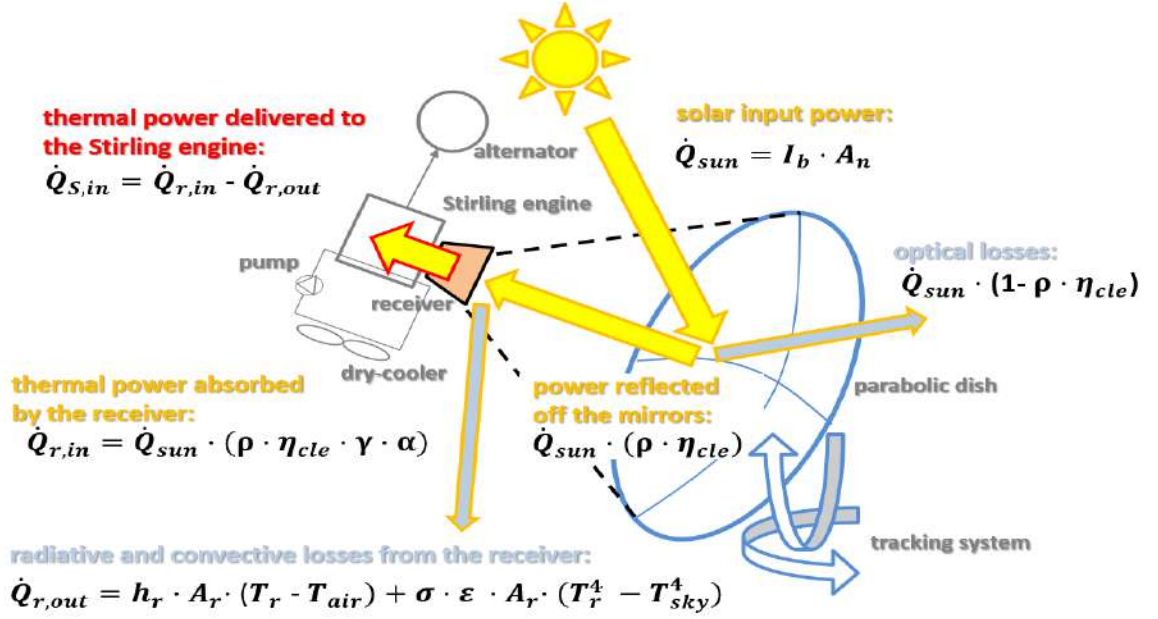


Figure II.5. Schematic diagram showing the energy balance of the solar collector [20].

Taking into account a combination of these effects, the concentrated solar power effectively absorbed by the cavity receiver is usually expressed as:

$$\dot{Q}_{r,in} = \dot{Q}_{sun} \cdot \eta_0 \quad (II.3)$$

Where:

$\dot{Q}_{r,in}$ : Thermal energy power absorbed by the receiver [W].

$\eta_0$ : Effective optical efficiency (dimensionless).

$$\eta_0 = \rho \cdot \eta_{cle} \cdot \gamma \cdot \alpha \quad (II.4)$$

Where:

$\rho$ : Clean mirror reflectance (dimensionless).

$\eta_{cle}$ : Cleanliness index of the collector mirror (dimensionless).

$\gamma$ : intercept factor of the solar collector (dimensionless).

$\alpha$ : Effective absorptivity of the receiver (dimensionless).

In other words, optical efficiency  $\eta_0$  can be interpreted as the ratio between solar power

absorbed by the receiver  $\dot{Q}_{r,in}$  and the rate of solar power hitting the collector, while the

intercept factor  $\gamma$  is the ratio between the rate of energy hitting the receiver  $\dot{Q}_{sun}$  and the

effective concentrated solar power reflected off the mirrors of the concentrator collector. The

intercept factor  $\gamma$ , in particular, incorporates the combination of errors associated with the

## Chapter II: A theoretical study of the stirling system

---

control of sun tracking, the erroneous positioning of the receiver and defocusing, due to wind-induced vibrations of the collector structures [20].

It is also necessary to consider the additional convective and radiative thermal losses from the aperture of the cavity receiver, due to the high temperatures reached at its internal surface.

$$\dot{Q}_{r,out} = \dot{Q}_{con} + \dot{Q}_{rad} \quad (II.5)$$

Where:

$\dot{Q}_{r,out}$  : Thermal losses from the receiver [W].

$\dot{Q}_{con}$  : Rate of thermal convective losses from the receiver [W].

$\dot{Q}_{rad}$  : Flux of radiant energy emitted from the receiver [W].

$$\dot{Q}_{con} = h_r \cdot A_r \cdot (T_r - T_{air}) \quad (II.6)$$

Where  $\dot{Q}_{con}$  and  $\dot{Q}_{rad}$  are the convective and radiative losses respectively [20].

Where:

$h_r$  : Natural convective coefficient at receiver surface [W/ (m<sup>2</sup> ·K)].

$A_r$  : Receiver equivalent surface area [m<sup>2</sup>].

$T_r$  : Temperature of the receiver surface [K].

$T_{air}$  : Air temperature [K].

$$\dot{Q}_{con} = h_r \cdot A_r \cdot (T_r - T_{air}) \quad (II.7)$$

Where:

$\sigma$  : Stefan–Boltzmann constant,  $5.67 \times 10^{-8}$  [W/ (m<sup>2</sup> · K<sup>4</sup>)]

$\varepsilon$  : Effective emissivity factor of the receiver (dimensionless)

$T_{sky}$  : Effective sky temperature [K]

## Chapter II: A theoretical study of the stirling system

---

This temperature depends on the atmospheric conditions and is usually related to the air temperature by empirical formulas like the following [20]:

$$T_{sky} = 0.0552 \cdot T_{air}^{1.5} \quad (II.8)$$

It is not trivial to observe that the greater the aperture of the cavity receiver  $A_r$ , the greater the thermal losses  $\dot{Q}_{r,out}$  and the higher the intercept factor  $\gamma$ . Thus, the correct design of the dimension of the receiver aperture should always be based on the trade-off between two opposing tendencies: the reduction of thermal loss from the receiver and the increase in optical efficiency, the latter being proportional to the intercept factor as shown in Eq. 4. From the energy balance of the receiver, it is possible to express the thermal power which is effectively delivered to the Stirling engine by the following difference [20]:

$$\dot{Q}_{S,in} = \dot{Q}_{r,in} - \dot{Q}_{r,out} \quad (II.9)$$

Which, using all of the above equations, can be recast as [20]:

$$\dot{Q}_{S,in} = I_b \cdot A_n \cdot \eta_0 - A_r \cdot [h_r \cdot (T_r - T_{air}) + \sigma \cdot \varepsilon \cdot (T_r^4 - T_{sky}^4)] \quad (II.10)$$

Where:

$\dot{Q}_{S,in}$  : Thermal power delivered to the Stirling engine [W].

$I_b$  : Solar beam radiation [W/m<sup>2</sup>].

Thus, dividing Eq. 9 by Eq. 1, it is possible to make explicit the expression describing the thermal efficiency of the solar collector as [20]:

$$\eta_c = \frac{\dot{Q}_{S,in}}{\dot{Q}_{sun}} = \eta_0 - \frac{1}{I_b \cdot C_g} \cdot [h_r \cdot (T_r - T_{air}) + \sigma \cdot \varepsilon \cdot (T_r^4 - T_{sky}^4)] \quad (II.11)$$

Where:

$\eta_c$  : Thermal efficiency of the solar collector (dimensionless).

Where  $C_g$  is the solar collector geometric concentration ratio defined as:

## Chapter II: A theoretical study of the stirling system

$$C_g = \frac{A_n}{A_r} \quad (\text{II.12})$$

$C_g$  : Geometric concentration ratio of the collector (dimensionless).

After calculating the thermal solar input power to the CSP system, the amount of this power that can be transformed into electrical power needs to be determined, but it is first necessary to evaluate the mechanical output power of the Stirling engine by exploiting the energy balance of the PCU (see Fig.II.6).

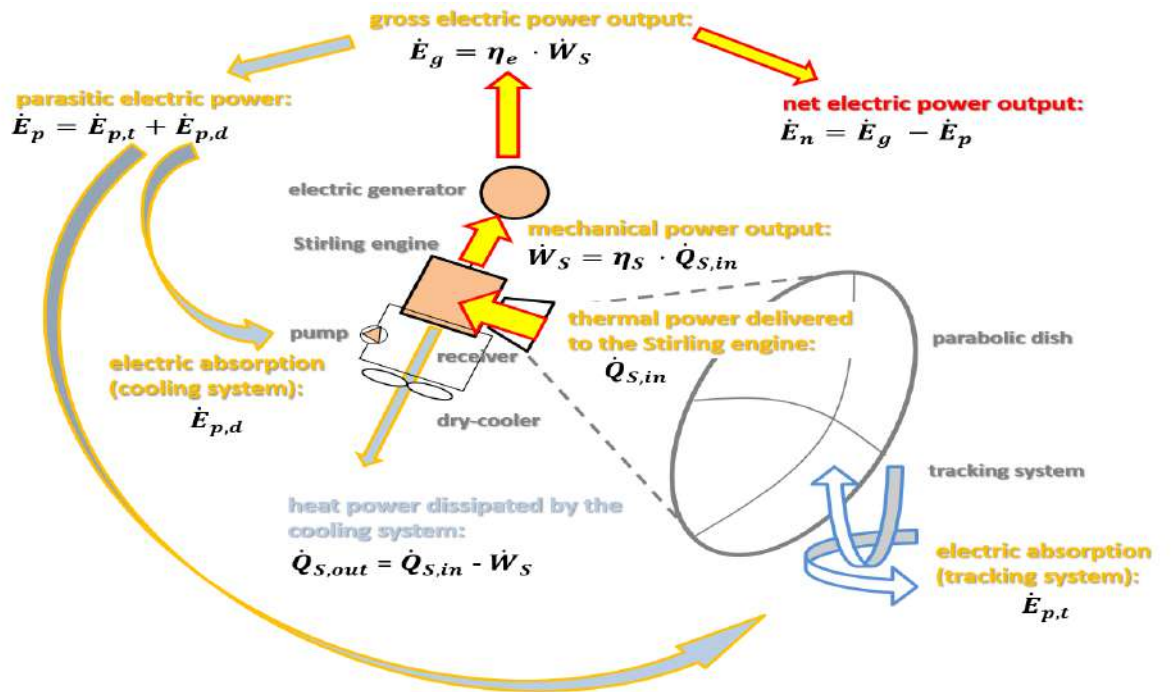


Figure II.6. Schematic diagram showing the energy balance of the PCU [20].

The mechanical output power of the Stirling engine is related to the input thermal power by the efficiency of the engine itself  $\eta_s$  as:

$$\dot{W}_S = \eta_s \cdot \dot{Q}_{S,in} \quad (\text{II.13})$$

Where:

$\dot{W}_S$  : Rate of mechanical work of the Stirling engine [W].

$\eta_s$  : Efficiency of the Stirling engine (dimensionless).



## ***Chapter II: A theoretical study of the stirling system***

---

From a theoretical point of view, the Stirling cycle consists of four internally reversible processes: two processes are isothermal compressions at temperature  $T_h$  and  $T_c$ ; the other two thermodynamic processes are isochoric (constant volume). During isothermal expansion at temperature  $T_h$ , heat is added to the working fluid, while during isothermal compression at temperature  $T_c$ , heat is rejected to the surroundings. A regenerator with full effectiveness allows the heat rejected during the isochoric rarefaction to be transferred during the isochoric compression. This Stirling cycle exhibits the same Carnot thermal efficiency. The efficiency of the Stirling engine, in turn, could be generally related to the reversible Carnot efficiency of the engine, between the same  $T_h$  and  $T_c$  limiting temperatures, as [20]:

$$\eta_S = \eta_{S,ex} \cdot \eta_{S,C} \quad (\text{II.14})$$

Where:

$\eta_{S,ex}$ : Energetic efficiency of the Stirling engine (dimensionless).

$\eta_{S,C}$ : Carnot cycle efficiency of the Stirling engine (dimensionless).

### **6.2. Carnot cycle efficiency of the Stirling engine**

$$\eta_{S,C} = 1 - \frac{T_c}{T_h} \quad (\text{II.15})$$

Where:

$T_h$ : Heat input temperature of the engine working fluid [K].

$T_c$ : Rejection temperature of the engine working fluid [K].

represents the ratio between the maximum theoretical mechanical power output of the ideal Stirling cycle operating between the limiting temperatures  $T_h$  and  $T_c$ , and the actual thermal power input  $\dot{Q}_{S,in}$ . The energetic efficiency  $\eta_{S,ex}$ , represents the ratio between the actual mechanical power output  $\dot{W}_S$  and the maximum mechanical power. The value of the energetic efficiency takes into account the irreversibility of the engine [20] and is found between  $\eta_{S,ex} = 0.55-0.88$  [20]. More generally, it is also necessary to consider that the performance of these kinds of systems depends on many factors, among which is the effect of the partialisation of

## Chapter II: A theoretical study of the stirling system

---

the input thermal power due to fluctuations in solar radiation. For solar dish-Stirling engines, it is often assumed  $\eta_{s,ex} = 0.5$ , though there are relatively few experimental works on the performance of these engines.

In addition, using the energy balance of the Stirling engine (see Fig.II.6), based on the assumption that the heat delivered to the Stirling engine and the heat dissipated  $\dot{Q}_{S,out}$  occur simultaneously, it is also possible to express the thermal power that must be dissipated by the cooling systems as[20]:

$$\dot{Q}_{S,out} = \dot{Q}_{S,in} - \dot{W}_S = (1 - \eta_s) \cdot \dot{Q}_{S,in} \quad (\text{II.16})$$

Where:

$\dot{Q}_{S,out}$  : Thermal power rejected from the Stirling engine [W].

Based both on the analysis of the real data of partial load operation of the original USAB 4-95 Stirling engine (working with  $T_h = 720$  °C) and on the performance of the Stirling engine of the SES plant, the author decided to approximate with a linear regression the curve between the thermal input power and the mechanical output power of the engine as [20]:

$$\dot{W}_S = (a_1 \cdot \dot{Q}_{S,in} - a_2) \cdot R_T \quad (\text{II.17})$$

Where:

$a_1$  : slope of the linear relation between  $\dot{W}_S$  and  $\dot{Q}_{S,in}$  (dimensionless).

$a_2$  : intercept of the linear the relationship between  $\dot{W}_S$  and  $\dot{Q}_{S,in}$  [W].

$R_T$  : Ratio of temperature  $T_0$  to temperature  $T_{air}$  (dimensionless).

### 6.3. Ratio of temperature

$$R_T = \frac{T_0}{T_{air}} \quad (\text{II.18})$$

Where:

$T_0$  : Reference temperature [K].

## Chapter II: A theoretical study of the stirling system

---

This last correction factor was introduced, inspired by what was proposed in the Stine model and similar ones, to take into account the effect of variations in outside temperature on the efficiency of the Stirling engine. Finally, combining Eq. 12 with Eq. 16, it follows [20]:

### 6.4. The efficiency of the Stirling engine

$$\eta_s = \left( a_1 - \frac{a_2}{\dot{Q}_{s,in}} \right) \cdot R_T \quad (\text{II.19})$$

Using the mechanical output power of the engine, it is then possible to evaluate the gross electric power of **PCU** by:

$$\dot{E}_g = \eta_e \cdot \dot{W}_s \quad (\text{II.20})$$

Where:

$\dot{E}_g$ : Gross electric output power [W].

$\eta_e$ : Average electric generator efficiency (dimensionless).

The net electric power of the **CSP** system can be determined by subtracting the total parasitic electric absorption  $\dot{E}_p$  from the electric gross power:

$$\dot{E}_n = \dot{E}_g - \dot{E}_p \quad (\text{II.21})$$

Where:

$\dot{E}_n$ : Net electric output power [W].

$\dot{E}_p$ : Total parasitic absorption power [W].

The total parasitic power of the dish-Stirling unit, in turn, is mostly the sum of two contributors: the electric absorption of the control system and tracking motors  $\dot{E}_{p,t}$  and those of the pumps and fans of the cooling system  $\dot{E}_{p,d}$ , i.e.:

$$\dot{E}_p = \dot{E}_{p,t} + \dot{E}_{p,d} \quad (\text{II.22})$$

$\dot{E}_{p,d}$ : Parasitic absorption power of the dry-cooler and circulation pumps [W].

$\dot{E}_{p,t}$ : Parasitic absorption power of the tracking system [W].

## Chapter II: A theoretical study of the stirling system

---

Finally, the instantaneous efficiency from solar-to-electric for all the dish-Stirling plants can be calculated as the ratio between the net electrical power produced and the solar power hitting the concentrator mirrors:

$$\eta_{DS} = \frac{\dot{E}_n}{\dot{Q}_{sun}} \quad (\text{II.23})$$

By substituting: the right-hand-side of Eq. 9 into Eq. 16 and, then the right-hand-side of the obtained expression into Eq. 19 and, finally, the resulting expression into Eq. 20, it is possible to obtain, in a compact form, the following equation:

$$\dot{E}_n = \eta_e \cdot \eta_0 \cdot a_1 \cdot A_n \cdot R_T \cdot I_b - [\eta_e \cdot a_1 \cdot \dot{Q}_{r,out} + a_2 \cdot R_T + \dot{E}_p] \quad (\text{II.24})$$

### 6.5. A linear model of dish-Stirling electric power generation

From the inspection of Eq. 4-7, using an appropriate set of parameters, it may easily be verified that, if the receiver temperature  $T_r$  is kept almost constant during plant operation (as, for example, observed in the measurements dataset of the dish-Stirling in Palermo), the thermal losses from the receiver are not very sensitive to variations in  $T_{air}$ . Under this assumption, it follows from Eq. 23, that the gross electric power output can be expressed as [20]:

$$\dot{E}_g = \eta_e \cdot \eta_0 \cdot a_1 \cdot A_n \cdot I_b - [\eta_e \cdot a_1 \cdot \dot{Q}_{r,out}^{ave} + a_2] \cdot R_T \quad (25)$$

Where:

$$\dot{Q}_{r,out}^{ave} : \text{Average value of the thermal losses from the receiver [W].}$$

That Eq. 24 simplifies to a linear relationship between the gross electrical power output and the solar beam radiation. Interestingly, this linearity emerges from the analysis of the operational data of existing dish-Stirling plants and is the basis of the empirical model proposed and validated by Stine [20].

As in the Stine model, Eq. 24 shows that the optical efficiency reduction due to the soiling of mirrors has the practical effect of changing the slope of the linear equation. Stine in particular introduces this effect through the corrected insolation concept defined as the product of the current beam radiation with a reflectance ratio; the latter defined as the ratio between the measured current reflectance (with soiled mirrors) and that with clean mirrors. On the other

## Chapter II: A theoretical study of the stirling system

---

hand, unlike the original Stine model, we have defined the correction term  $R_T$  in Eq. 23 in analogy to what is proposed in the Sandia National Laboratories model for SES dish-Stirling plants, i.e., as a ratio between a rated temperature and the current air temperature (see Eq. 17).

Moreover, if we further assume a constant value for the parasitic absorptions, equal to the average of the values measured during the operation of the plant  $\dot{E}_p^{ave}$ , we can obtain from Eq. 24[20]:

### 6.6. The net output power generated by the plant and the normal direct radiation hitting the collector mirrors

$$\dot{E}_n = \eta_e \cdot \eta_0 \cdot a_1 \cdot A_n \cdot R_T \cdot I_b - [\eta_e \cdot a_1 \cdot \dot{Q}_{r,out}^{ave} + a_2 \cdot R_T + \dot{E}_p^{ave}] \quad (26)$$

Where:

$\dot{E}_p^{ave}$  : Average value of the total parasitic absorption power [W].

In addition, this linearity has been extensively observed by the experimental performance data of numerous dish-Stirling plants operating with clean mirrors [20].

To this end, we can further simplify Eq. 25 assuming an average value of the ambient temperature  $T_{air}^{ave}$  and, therefore, an average value of the corrector factor  $R_T^{ave}$ , obtaining:

$$\dot{E}_n = b_1 \cdot I_b - b_2 \quad (27)$$

Where:

$b_1$  : slope of the linear relationship between  $\dot{E}_n$  and  $I_b$  [ Kw · m<sup>2</sup> /W].

$b_2$  : intercept of the linear relationship between  $\dot{E}_n$  and  $I_b$  [W].

Where the slope is equal

$$b_1 = \eta_e \cdot \eta_0 \cdot a_1 \cdot A_n \cdot R_T^{ave} \cdot 10^{-3} \quad (28)$$

In addition, the intercept is equal to

## Chapter II: A theoretical study of the stirling system

---

$$b_2 = \eta_e \cdot a_1 \cdot \dot{Q}_{r,out}^{ave} + a_2 \cdot R_T^{ave} + \dot{E}_p^{ave} \quad (29)$$

Where:

$R_T^{ave}$  : Average value of the ratio of temperature  $T_0$  to temperature  $T_{air}$  (dimensionless).

### 6.7. The thermal losses from the receiver

$$\dot{Q}_{r,out}^{ave} = \alpha \cdot \rho \cdot \gamma \cdot I_b^{\max} - \dot{Q}_{S,in}^{\max} \quad (30)$$

Where:

$I_b^{\max}$  : Maximum design value of the solar beam radiation [W/m<sup>2</sup>].

$\dot{Q}_{S,in}^{\max}$  : Maximum design value of the thermal power delivered to the Stirling engine [W].

Finally, from Eq. 27, it is possible to calculate:

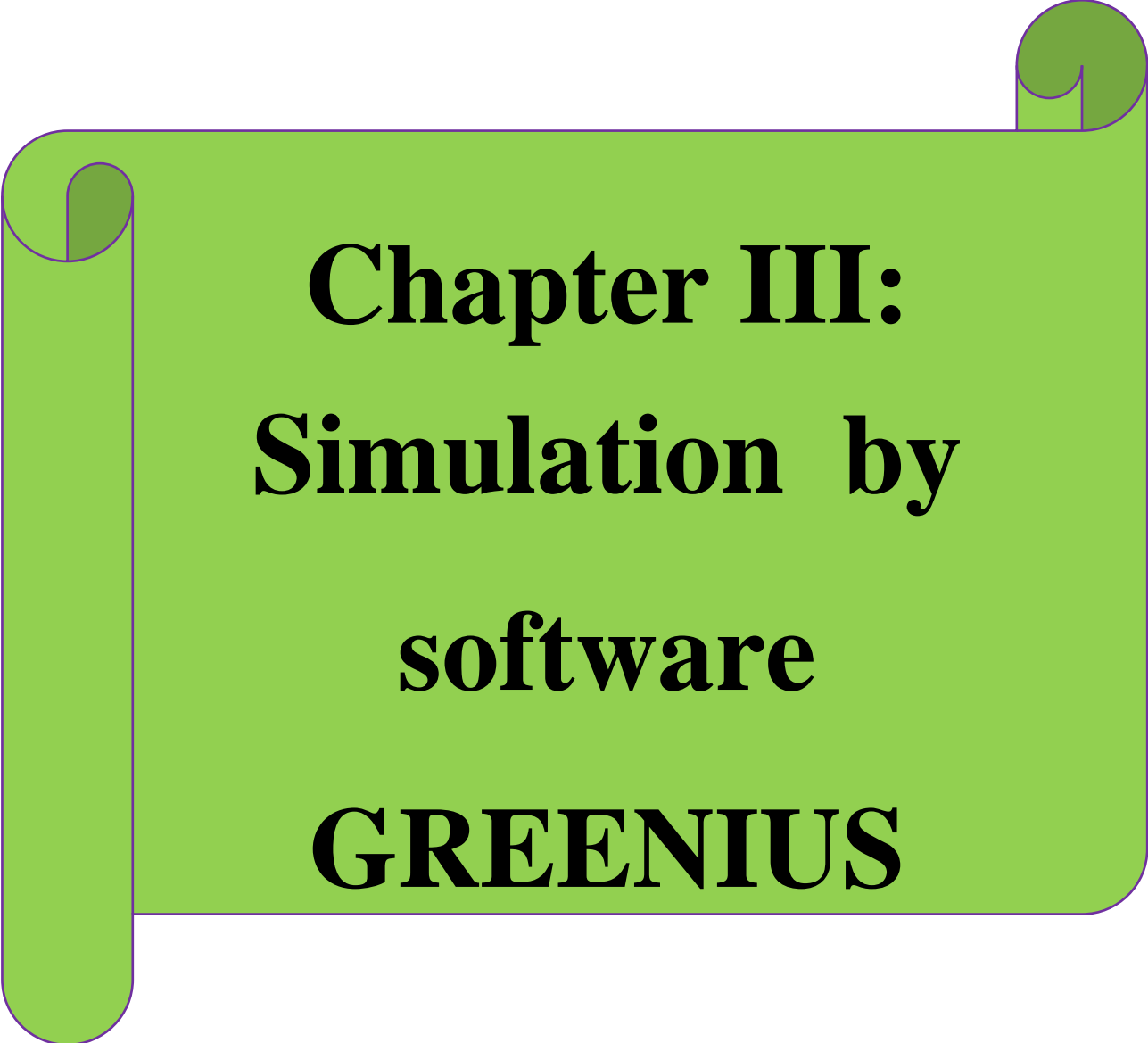
$$a_1 = 10^3 \cdot \frac{b_1}{\eta_e \cdot \eta_0 \cdot A_n \cdot R_T^{ave}} \quad (31)$$

In addition, after introducing Eq. 30 in Eq. 28:

$$a_2 = \frac{[b_2 - \dot{E}_p^{ave} \cdot \eta_0 \cdot A_n - 10^3 \cdot b_1 \cdot \dot{Q}_{r,out}^{ave}]}{\eta_e \cdot \eta_0 \cdot A_n \cdot R_T^{ave}} \quad (32)$$

## 7. Chapter summary:

After studying the workings of the Stirling engine, describing the system and providing an overview of Greenius and System Advisor Model software, learning about engine mechanics and the power cycle, we finally touched on the various laws and mathematical relationships related to the solar dish. From this point of view, we will conduct an empirical study to discuss and analyze that study, so we have prepared a project, which is the solar dish model, in addition to using Energy3D simulation software, Greenius and System Advisor Model, which shows the most important previous studies of the solar dish complex.



**Chapter III:  
Simulation by  
software  
GREENIUS**

### 1 An introduction

In this chapter, we will discuss the study of the electrical energy productivity of 5 dish Stirling systems for some states of the east, west, north and south of Algeria, through the use of simulation programs GREENIUS and comparing the results.

### 2 Simulation by software GREENIUS

#### 2.1 The Northern States

##### 2.1.1 Dish output (E-grid):

The following table represents the production of the dish output for 5 solar dishes in the northern Algerian states.

	Alger (kWh)	Annaba (kWh)	Bejaïa (kWh)	Jijel (kWh)	Skikda (kWh)
January	2 103	3 614	4 709	3 393	3 917
February	3 344	3 235	3 763	3 906	3 265
March	3 887	5 029	5 187	4 082	5 218
April	5 307	4 762	5 329	6 317	5 566
May	5 948	6 400	5 688	6 786	7 309
June	6 576	8 061	7 813	7 952	8 891
July	<b>8 296</b>	<b>9 215</b>	<b>8 993</b>	<b>9 864</b>	<b>11 103</b>
August	6 185	8 109	7 348	7 246	7 365
September	5 233	6 652	5 547	6 578	5 653
October	3 483	6 066	4 221	4 946	5 077
November	2 770	4 634	4 874	3 820	3 660
December	2 954	4 254	4 011	3 205	4 142

Table III.1: dish output of the northern states of Algeria



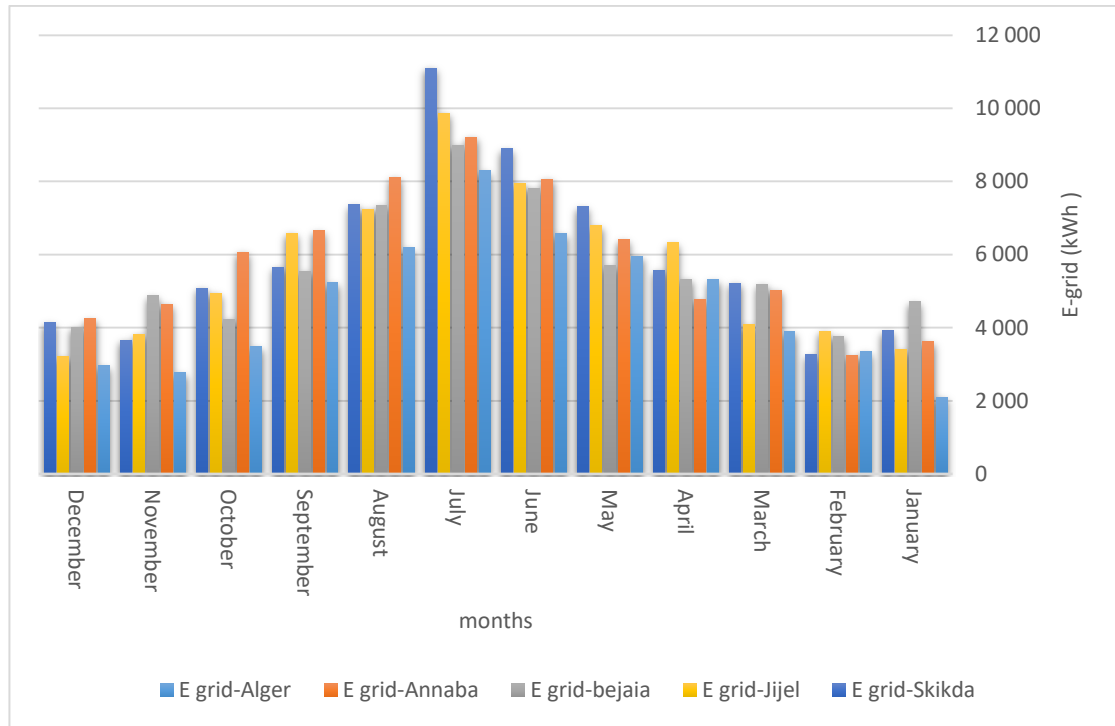


Figure III.1: dish output of the northern states of Algeria

### 2.1.2 Analysis and discussion

The columns represent the changes of dish output in terms of the months of the northern states of Algeria, where we note that the best northern state is the state of Skikda compared to other states, where it reached its maximum value estimated at 11103 kWh followed directly by the state of Jijel and estimated at 9684 kWh, followed by each of Annaba with 9215 kWh, then Bejaïa with 8993 kWh and Algeria with 8296 kWh on the order and this is during the month of July.

### 2.2 Irradiation on dish area (H-sol)

The following table represents the production of irradiation on dish area for 5 solar dishes in the northern Algerian states.

	H sol-Alger (kWh)	H sol-Annaba (kWh)	H sol-Bejaïa (kWh)	H sol-Jijel (kWh)	H sol-Skikda (kWh)
January	19 037	28 527	32 578	26 288	28 667
February	24 752	25 573	27 507	27 230	24 839
March	30 748	37 088	35 356	31 159	36 003

April	38 333	37 008	38 278	42 045	40 948
May	44 113	47 347	42 642	46 660	50 854
June	47 504	55 125	53 948	54 850	58 947
July	<b>58 180</b>	<b>61 051</b>	<b>61 133</b>	<b>65 053</b>	<b>70 535</b>
August	46 464	55 735	51 897	52 413	53 366
September	39 460	46 629	39 737	44 473	41 508
October	28 522	41 659	33 331	35 466	35 532
November	21 144	34 052	33 147	27 510	27 785
December	23 902	31 415	30 379	25 645	30 663

Table III.2: irradiation on dish area of the northern states of Algeria

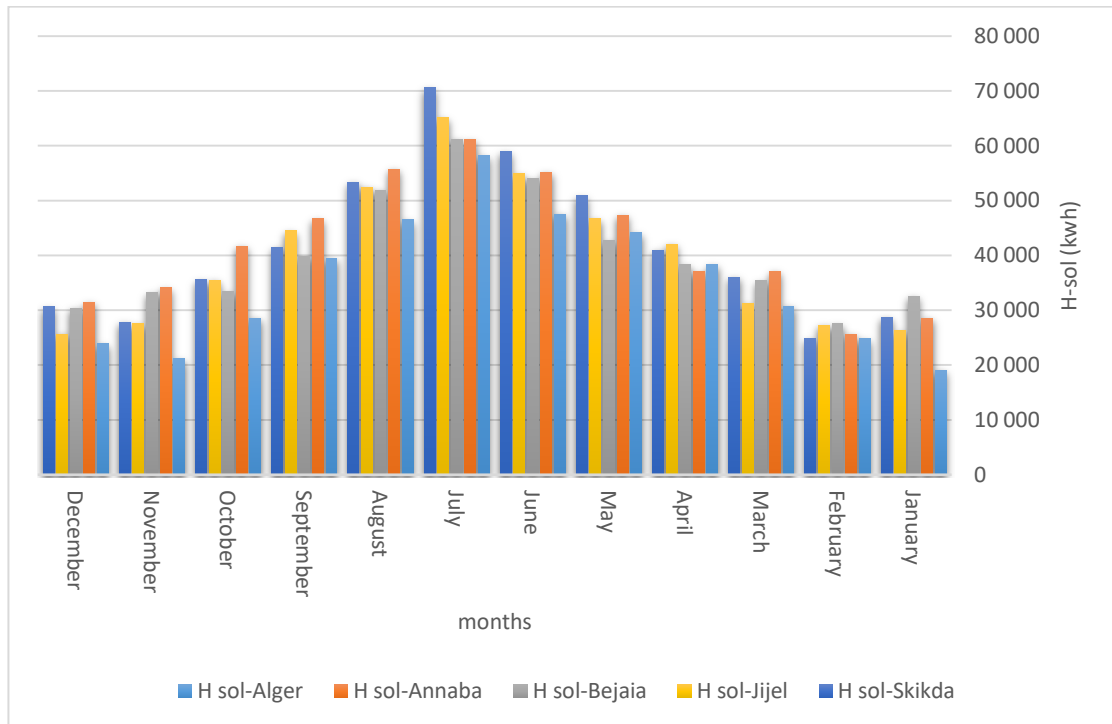


Figure III.2: Irradiation on dish area of the northern states of Algeria

### 2.2.1 Analysis and discussion

The columns represent the changes of irradiation on dish area in terms of the months of the northern states of Algeria, where we note that the best northern state is the state of Skikda compared to other states, where it reached its maximum value estimated at 70535 kWh followed directly by the state of Jijel and estimated at 65053 kWh, followed by each of

### Chapter III: Simulation by software GREENIUS

Bejaïa with 61133 kWh, then Annaba with 61051 kWh and Algeria with 58180 kWh on the order and this is during the month of July.

The following table represents the technical results of electric power plant using 5 solar dishes in the northern Algerian states.

Technical Key Results	Alger	Annaba	Bejaïa	Jijel	Skikda
Meteorological Data:					
<b>Global horizontal irradiance (GHI)</b>	<b>1651.23</b>	<b>1789.08</b>	<b>1717.19</b>	<b>1714.55</b>	<b>1754.54kWh/ (m<sup>2</sup>·a)</b>
<b>Direct normal irradiance (DNI)</b>	<b>1489.10</b>	<b>1767.93</b>	<b>1692.89</b>	<b>1688.86</b>	<b>1762.43kWh/ (m<sup>2</sup>·a)</b>
Diffuse horizontal irradiance (Diff)	742.32	710.15	705.85	689.09	682.31kWh/ (m <sup>2</sup> ·a)
Mean Annual ambient temperature	16.74	17.56	17.98	18.61	18.09°C
Site Position and Orientation:					
Site	Default	Default	Default	Default	Default
Latitude	36.75	36.92	36.72	36.83	36.88 °N
Longitude	3.00	7.77	5.07	5.78	6.90 °E
Dish/Stirling System Characteristics:					
Installed capacity	0.05	0.05	0.05	0.05	0.05 MW
Number of units	5	5	5	5	5
Capacity per System	10.00	10.00	10.00	10.00	10.00 kW
Simulation Results:					
Total annual net elect. Output	56.09	70.03	67.48	68.09	71.17MWh
Total annual gross elect. Output	62.76	77.80	74.84	75.47	78.67MWh
Mean system efficiency	13.29	13.97	14.06	14.22	14.24 %

Table III.3: Technical Key Results of the northern states of Algeria

The following table represents the economic results of electric power plant using 5 solar dishes in the northern Algerian states.

Economic Key Results	Alger	Annaba	Bejaïa	Jijel	Skikda
----------------------	-------	--------	--------	-------	--------

### Chapter III: Simulation by software GREENIUS

Financial Input Parameters:					
Electricity Tariff	0.1700	0.1700	0.1700	0.1700	0.1700 €/kWh
Grant Proportion (Renewable)	0.00	0.00	0.00	0.00	0.00 %
Debt-Equity-Ratio	70.00	70.00	70.00	70.00	70.00 %
Average Interest Rate	5.64	5.64	5.64	5.64	5.64 %
Simulation Results:					
<b>Internal Rate of Return (IRR) on Equity</b>	<b>-24.50</b>	<b>-19.92</b>	<b>-20.55</b>	<b>-20.39</b>	<b>-19.65 %</b>
Net Present Value	-733,919	-713,904	-717,562	-716,687	-712,277 €
Payback Period	0.00	0.00	0.00	0.00	0.00 yrs.
Discounted Payback Period	0.00	0.00	0.00	0.00	0.00 yrs.
Total Incremental Costs	842,539	833,625	835,254	834,865	832,901 €
Minimum ADSCR	-0.20	-0.11	-0.13	-0.12	-0.10
Required Tariff (LCOE)	2.3132	1.8525	1.9226	1.9053	1.8231 €/kWh
Incremental LEC	1.1751	0.9312	0.9682	0.9591	0.9155 €/kWh
Calculation of LEC					
<b>Levelized Electricity Costs (LEC)</b>	<b>1.2251</b>	<b>0.9812</b>	<b>1.0182</b>	<b>1.0091</b>	<b>0.9655 €/kWh</b>
<b>Total Investment Costs (IC)</b>	<b>782,512</b>	<b>782,512</b>	<b>782,512</b>	<b>782,512</b>	<b>782,512 €</b>
Annuity of IC	0.08	0.08	0.08	0.08	0.08
NPV of Running Costs (OC)	95,875	95,875	95,875	95,875	95,875€
Annuity of OC	0.08	0.08	0.08	0.08	0.08
Environmental Aspects:					
<b>Annual CO2 Reduction</b>	<b>33.65</b>	<b>42.02</b>	<b>40.49</b>	<b>40.86</b>	<b>42.70 t CO2</b>

Table III.4: Economic Key Results of the northern states of Algeria

### 2.3 Interpretation

Skikda advantage back in terms of electricity production compared to Annaba and Jijel, Algeria and Bejaïa because they contain a higher proportion of total annual net electricity output estimated at 71.17 MWh and total annual gross electricity output at 78.67 MWh, allowing them to get the best year this production technically either in terms of side economic

## Chapter III: Simulation by software GREENIUS

---

characterized Skikda less value Levelized electricity costs and also maintain generally to reduce the proportion carbon dioxide emissions at 42.70t CO<sub>2</sub> and this is shown in both tables technical and economic key results.

### 3 The eastern states

#### 3.1 Dish output

The following table represents the production of the dish output for 5 solar dishes in the eastern Algerian states.

	Biskra (kWh)	Bordj Bou Arreridj (kWh)	Constantine (kWh)	Guelma (kWh)	Batna (KWh)
January	8 150	6 671	4 888	2 111	6 496
February	6 570	5 699	5 250	2 350	6 069
March	10 180	8 497	6 763	2 148	8 250
April	9 558	8 294	7 696	2 762	8 312
May	9 758	10 189	8 918	2 540	10 273
June	9 170	11 124	10 742	1 829	10 999
July	<b>10 823</b>	<b>13 560</b>	<b>13 471</b>	2 645	<b>13 976</b>
August	8 903	11 922	10 680	<b>3 184</b>	11 922
September	6 842	8 236	7 957	3 168	9 089
October	6 229	8 351	6 487	2 806	8 018
November	8 384	6 372	5 483	2 588	7 448
December	7 611	6 848	5 843	2 829	6 582

Table III.5: dish output of the eastern states

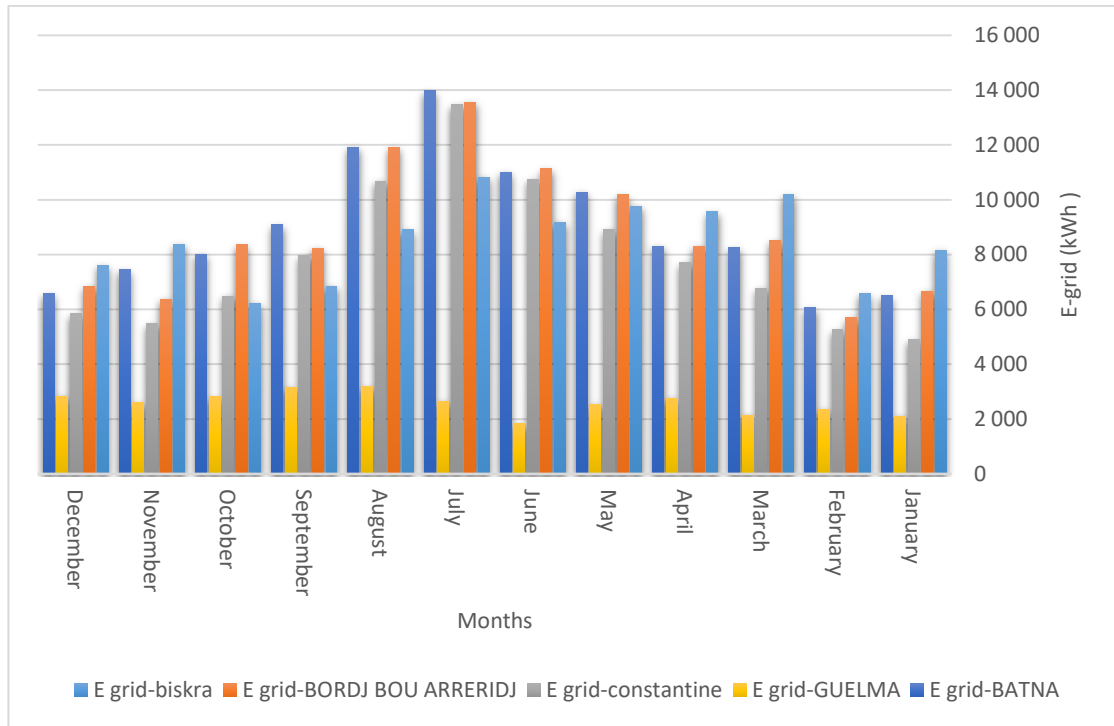


Figure III.3: Dish output of the eastern states of Algeria

### 3.1.1 Analysis and discussion

Columns graphs represent changes dish output in terms of months, where Batna the highest recorded value of the production of electrical energy compared to all of Guelma and Biskra and Constantine and Bordj Bou Arreridj estimated at 13976 kWh followed by the state of Bordj Bou Arreridj at 13560 kWh and then the state of Constantine at 13471 kWh Constantine followed by Biskra to 10830 kWh respectively. This in the month of July either Guelma province it has recorded the highest production value in the month of August was estimated at 3184 kWh.

### 3.2. Irradiation on dish area (H-sol)

The following table represents the production of irradiation on dish area for 5 solar dishes in the eastern Algerian states.

	H sol-Biskra (kWh)	H sol-Bordj Bou Arreridj (kWh)	H sol- Constantine (kWh)	H sol- Guelma (kWh)	H sol- Batna (kWh)
January	49 759	42 481	33 733	17 831	41 441
February	43 536	37 313	33 287	19 175	39 827

March	60 948	51 936	43 893	19 131	52 211
April	59 719	52 165	49 382	21 863	52 662
May	64 619	62 495	58 391	20 682	64 087
June	61 857	68 904	67 101	16 663	68 459
July	<b>70 300</b>	<b>81 090</b>	<b>81 071</b>	20 171	<b>82 877</b>
August	60 642	72 702	67 706	23 718	73 034
September	48 368	52 096	51 317	<b>24 977</b>	55 243
October	44 832	51 466	43 766	22 092	51 067
November	50 760	40 895	36 753	20 950	44 826
December	47 410	41 235	37 317	21 639	40 893

Table III.6: irradiation on dish area of the eastern states of Algeria

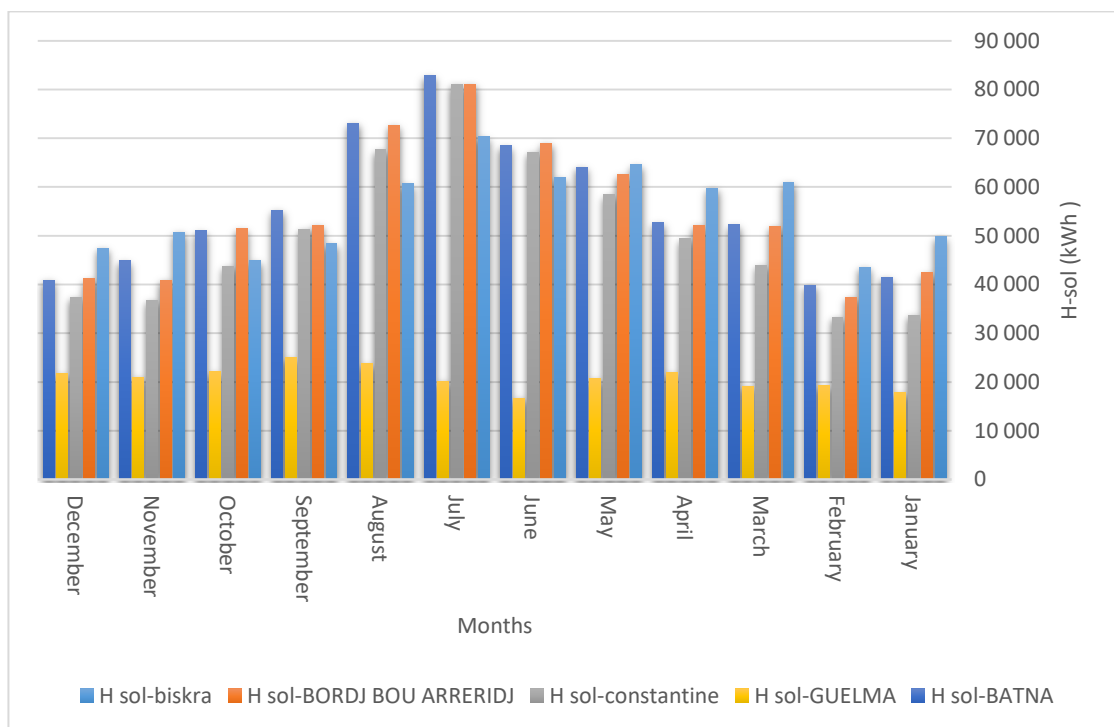


Figure III.4: irradiation on dish area of the eastern states of Algeria

### 3.2.1 Analysis and discussion

Columns graphs represent changes irradiation on dish area in terms of months, where Batna the highest recorded value of the production of electrical energy compared to all of Guelma and Biskra and Constantine and Bordj Bou Arreridj estimated at 82877 kWh followed by the

### Chapter III: Simulation by software GREENIUS

state of Bordj Bou Arreridj at 81090 kWh and then the state of Constantine at 81071 kWh followed by Biskra to 70300 kWh respectively. This in the month of July either Guelma province it has recorded the highest production value in the month of September was estimated at 24977 kWh.

The following table represents the technical results of electric power plant using 5 dishes in the eastern Algerian states.

Technical Key Results	Biskra	Bordj Bou Arreridj	Constantine	Guelma	Batna
Meteorological Data :					
<b>Global horizontal irradiance (GHI)</b>	<b>2016.83</b>	<b>1925.29</b>	<b>1875.06</b>	<b>1405.58</b>	<b>1953.54 kWh/ (m<sup>2</sup>·a)</b>
<b>Direct normal irradiance (DNI)</b>	<b>2337.74</b>	<b>2309.63</b>	<b>2129.51</b>	<b>877.93</b>	<b>2351.43 kWh/ (m<sup>2</sup>·a)</b>
Diffuse horizontal irradiance (Diff)	596.12	543.11	596.29	842.91	548.08 kWh/ (m <sup>2</sup> ·a)
Mean Annual ambient temperature	22.76	15.95	15.91	21.51	15.62°C
Site Position and Orientation :					
Site	Default	Default	Default	Default	Default
Latitude	34.80	36.07	36.28	21.33	35.57°N
Longitude	5.73	4.77	6.62	103.90	6.17°E
Dish/Stirling System Characteristics :					
Installed capacity	0.05	0.05	0.05	0.05	0.05 MW
Number of units	5	5	5	5	5
Capacity per System	10.00	10.00	10.00	10.00	10.00 kW
Simulation Results:					
Total annual net elect. output	102.18	105.76	94.18	30.96	107.43 MWh
Total annual gross elect. output	111.41	114.27	102.39	35.56	115.96 MWh
Mean system efficiency	15.42	16.15	15.60	12.44	16.12%

Table III.7: Technical key results of the eastern states of Algeria



### Chapter III: Simulation by software GREENIUS

The following table represents the economic results of electric power plant using 5 dishes in the eastern Algerian states.

Economic Key Results	Biskra	Bordj Bou Arreridj	Constantine	Guelma	Batna
Financial Input Parameters :					
Electricity Tariff	0.1700	0.1700	0.1700	0.1700	0.1700 €/kWh
Grant Proportion (Renewable)	0.00	0.00	0.00	0.00	0.00 %
Debt-Equity-Ratio	70.00	70.00	70.00	70.00	70.00 %
Average Interest Rate	5.64	5.64	5.64	5.64	5.64 %
Simulation Results :					
<b>Internal Rate of Return (IRR) on Equity</b>	<b>-14.75</b>	<b>-14.34</b>	<b>-15.73</b>	<b>-180.27</b>	<b>-14.16 %</b>
Net Present Value	-667,771	-662,626	-679252	-769977	-660229 €
Payback Period	0.00	0.00	0.00	0.00	0.00 yrs
Discounted Payback Period	0.00	0.00	0.00	0.00	0.00 yrs
Total Incremental Costs	813,079	810,787	818192	858599	809720 €
Minimum ADSCR	0.05	0.06	0.03	-0.35	0.06
Required Tariff (LCOE)	1.2698	1.2267	1.3776	4.1904	1.2076 €/kWh
Incremental LEC	0.6225	0.5997	0.6796	2.1694	0.5896 €/kWh
Calculation of LEC					
<b>Levelized Electricity Costs (LEC)</b>	<b>0.6725</b>	<b>0.6497</b>	<b>0.7296</b>	<b>2.2194</b>	<b>0.6396 €/kWh</b>
<b>Total Investment Costs (IC)</b>	<b>782,512</b>	<b>782,512</b>	<b>782512</b>	<b>782512</b>	<b>782512 €</b>
Annuity of IC	0.08	0.08	0.08	0.08	0.08
NPV of Running Costs (OC)	95,875	95,875	95875	95875	95875 €
Annuity of OC	0.08	0.08	0.08	0.08	0.08
Environmental Aspects :					
<b>Annual CO2 Reduction</b>	<b>61.31</b>	<b>63.46</b>	<b>56.51</b>	<b>18.58</b>	<b>64.46 t CO<sub>2</sub></b>

Table III.8: Economic key results of the eastern states of Algeria

### 3.3 Interpretation

Favorable state of return of Batna from the rest of the eastern states in direct normal irradiance reaching a maximum 2351.43 kWh/m<sup>2</sup> as it is the coldest east where area temperature reached the 15.62°C compared with other states and the cost of production in less than Guelma and Biskra and Constantine and Bordj Bou Arreridj, which best position to be the state in terms of production and also contributes in major to reduce the proportion of carbon dioxide emissions by 64.46 t CO<sub>2</sub>. This is illustrated in the table's technical and economic key results.

## 4. The southern states

### 4.1 Dish output (E-grid):

The following table represents the production of the dish output for 5 solar dishes in the southern Algerian states.

	Adrar (kWh)	Ghardaïa (kWh)	In-Saleh (kWh)	Tamanrasset (kWh)	Ouargla (kWh)
January	<b>12 398</b>	10 839	<b>12 773</b>	<b>11 564</b>	4 646
February	10 136	9 927	9 808	11 344	3 769
March	12 395	12 690	11 336	12 018	3 970
April	12 294	<b>12 700</b>	10 983	11 108	3 537
May	11 442	12 175	10 603	9 462	4 464
June	11 093	11 937	10 599	11 048	3 815
July	10 979	12 647	11 114	10 622	3 763
August	10 978	10 904	11 345	9 374	4 236
September	9 328	9 740	8 756	7 850	4 330
October	9 218	9 438	9 145	10 067	4 999
November	10 751	10 317	10 179	8 526	4 773
December	11 429	10 075	10 488	9 172	<b>5 064</b>

Table III.9: Dish output of the southern states of Algeria

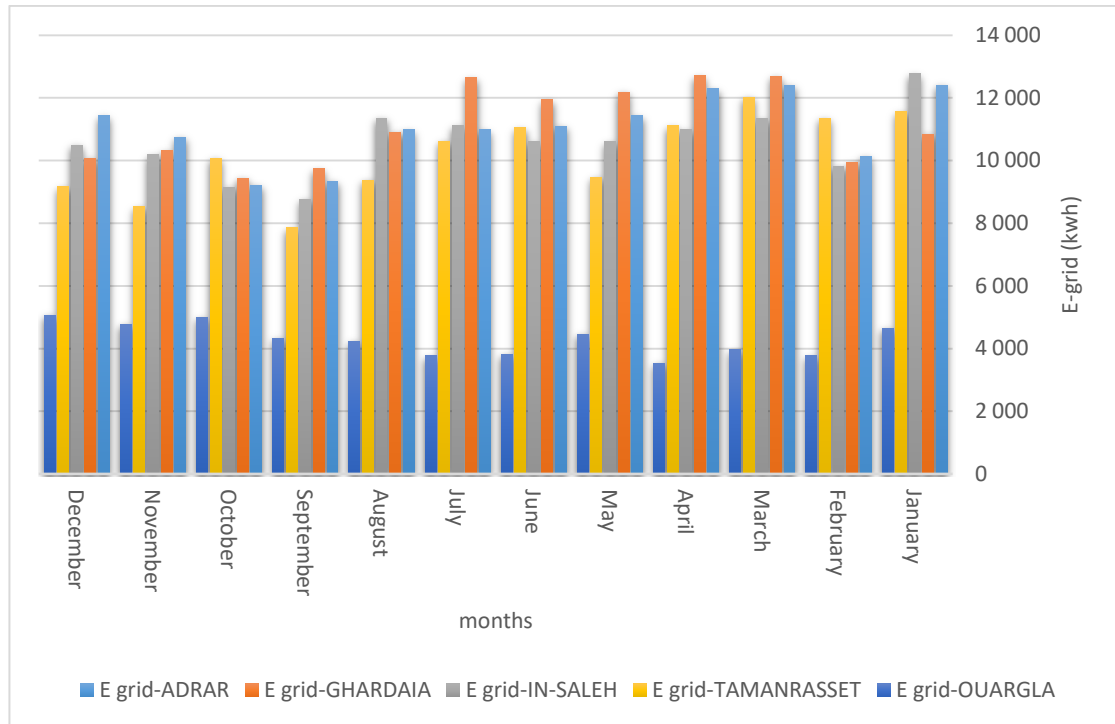


Figure III.5: Dish output of the southern states of Algeria

#### 4.1.1 Analysis and discussion

Columns graphs represent changes dish output in terms of months, where In-Saleh recorded the highest value of electrical energy production compared to all of Ouargla and Adrar and Tamanrasset and Ghardaïa estimated at 12773 kWh in January, followed by the state of Ghardaïa with 12700 kWh in April and then the state of Adrar with 12398 kWh in January, followed by Tamanrasset with 12018 kWh in March, followed by state of Ouargla with 5064 kWh in December.

#### 4.2 Irradiation on dish area (H-sol)

The following table represents the production of irradiation on dish area for 5 solar dishes in the southern Algerian states.

	Adrar (kWh)	Ghardaïa (kWh)	In-Saleh (kWh)	Tamanrasset (kWh)	Ouargla (KWh)
January	71 723	63 042	73 598	68 351	36 944
February	59 352	57 904	57 605	68 003	31 211
March	72 641	72 590	67 195	72 882	31 386
April	73 561	74 799	67 382	68 158	30 286

May	70 412	74 893	67 322	61 488	36 442
June	68 748	73 929	68 160	68 420	32 688
July	69 584	<b>78 171</b>	70 105	67 559	30 251
August	69 628	69 053	71 292	60 419	33 628
September	59 673	60 437	57 237	52 335	35 552
October	57 721	58 746	58 260	62 246	38 838
November	63 395	59 638	59 512	54 010	36 827
December	66 447	58 402	61 021	56 969	<b>39 325</b>

Table III.10: Irradiation on dish area of the southern states of Algeria

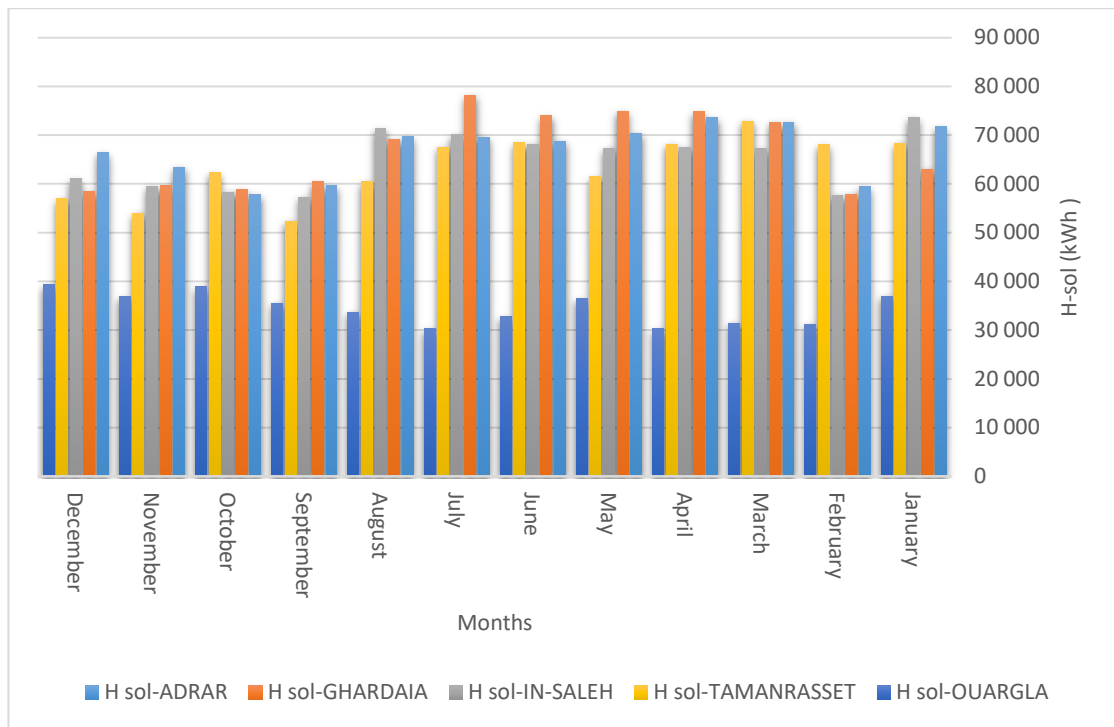


Figure III.6: Irradiation on dish area of the southern states of Algeria

#### 4.2.1 Analysis and discussion

Columns graphs represent changes Irradiation on dish area in terms of months, where Ghardaïa recorded the highest value of electrical energy production compared to all of Ouargla and Adrar and Tamanrasset and In-Saleh estimated at 78171 kWh in July, followed by the state of In-Saleh with 73598 kWh in January and then the state of Adrar with 73561 kWh in April, followed by Tamanrasset with 72882 kWh in March, followed by state of Ouargla with 36944 kWh in January.

### Chapter III: Simulation by software GREENIUS

The following table represents the technical results of electric power plant using 5 dishes in the southern Algerian states.

Technical Key Results	Adrar	Ghardaïa	In-Saleh	Tamanrasset	Ouargla
Meteorological Data :					
<b>Global horizontal irradiance (GHI)</b>	<b>2296.85</b>	<b>2210.58</b>	<b>2288.72</b>	<b>2362.59</b>	<b>2012.60 kWh/(m<sup>2</sup>·a)</b>
<b>Direct normal irradiance (DNI)</b>	<b>2832.05</b>	<b>2827.52</b>	<b>2746.70</b>	<b>2683.74</b>	<b>1458.12 kWh/(m<sup>2</sup>·a)</b>
Diffuse horizontal irradiance (Diff)	504.04	463.35	530.33	605.82	971.42kWh/(m <sup>2</sup> ·a)
Mean Annual ambient temperature	25.84	22.55	27.08	21.61	30.1°C
Site Position and Orientation :					
Site	Default	Default	Default	Default	Default
Latitude	27.82	32.40	27.20	22.78	5.00 °N
Longitude	-0.18	3.80	2.47	5.52	32.00 °E
Dish/Stirling System Characteristics :					
Installed capacity	0.05	0.05	0.05	0.05	0.05MW
Number of units	5	5	5	5	5
Capacity per System	10.00	10.00	10.00	10.00	10.00 kW
Simulation Results:					
Total annual net elect. output	132.44	133.39	127.13	122.15	51.37MWh
Total annual gross elect. output	142.38	143.24	136.94	131.40	58.18MWh
Mean system efficiency	16.50	16.64	16.33	16.06	12.43%

Table III.11: Technical key results of the southern states of Algeria

The following table represents the economic results of electric power plant using 5 dishes in the southern Algerian states.

Economic Key Results	Adrar	Ghardaïa	In-Saleh	Tamanrasset	Ouargla
Financial Input Parameters :					
Electricity Tariff	0.1700	0.1700	0.1700	0.1700	0.1700 €/kWh

### Chapter III: Simulation by software GREENIUS

Grant Proportion (Renewable)	0.00	0.00	0.00	0.00	0.00 %
Debt-Equity-Ratio	70.00	70.00	70.00	70.00	70.00 %
Average Interest Rate	5.64	5.64	5.64	5.64	5.64 %
Simulation Results :					
<b>Internal Rate of Return (IRR) on Equity</b>	<b>-11.82</b>	<b>-11.74</b>	<b>-12.27</b>	<b>-12.71</b>	<b>-27.35 %</b>
Net Present Value	-624,341	-622,979	-631,963	-639,105	-740.693€
Payback Period	0.00	0.00	0.00	0.00	0.00 yrs.
Discounted Payback Period	0.00	0.00	0.00	0.00	0.00 yrs.
Total Incremental Costs	793,736	793,129	797,130	800,311	845.557 €
Minimum ADSCR	0.11	0.11	0.10	0.09	-0.23
Required Tariff (LCOE)	0.9796	0.9727	1.0205	1.0621	2.5259 €/kWh
Incremental LEC	0.4688	0.4651	0.4905	0.5125	1.2877 €/kWh
Calculation of LEC					
<b>Levelized Electricity Costs (LEC)</b>	<b>0.5188</b>	<b>0.5151</b>	<b>0.5405</b>	<b>0.5625</b>	<b>1.3377 €/kWh</b>
<b>Total Investment Costs (IC)</b>	<b>782,512</b>	<b>782,512</b>	<b>782,512</b>	<b>782,512</b>	<b>782.512 €</b>
Annuity of IC	0.08	0.08	0.08	0.08	0.08
NPV of Running Costs (OC)	95,875	95,875	95,875	95,875	95.875€
Annuity of OC	0.08	0.08	0.08	0.08	0.08
Environmental Aspects :					
<b>Annual CO2 Reduction</b>	<b>79.46</b>	<b>80.03</b>	<b>76.28</b>	<b>73.29</b>	<b>30.82 t CO2</b>

Table III.12: Economic key results of the southern states of Algeria

### 4.3 Interpretation

The preference of the state of In-Saleh in the curves and columns of dish output is due to its position above the global horizontal irradiance, and the preference for the state of Ghardaïa is higher because it has higher direct normal irradiation.

**5 The western states**

**5.1 Dish output (E-grid):**

The following table represents the production of the dish output for 5 solar dishes in the western Algerian states.

	El-Bayadh (kWh)	Chlef (kWh)	Tiaret (kWh)	Tlemcen (kWh)	Oran (kWh)
January	6 441	5 801	3 393	6 608	2 401
February	6 498	5 036	3 906	5 008	4 462
March	8 325	6 925	4 082	7 403	5 088
April	7 870	6 995	6 317	7 236	7 888
May	10 919	8 228	6 786	9 182	<b>8 645</b>
June	10 752	10 500	7 952	9 968	6 412
July	<b>13 456</b>	<b>12 358</b>	<b>9 864</b>	<b>12 368</b>	7 166
August	12 423	10 077	7 246	10 502	6 795
September	8 379	7 824	6 578	8 651	8 347
October	7 791	7 197	4 946	7 657	5 603
November	7 232	6 114	3 820	7 134	4 544
December	6 378	4 961	3 206	6 039	4 738

Table III.13: Dish output of the western states of Algeria

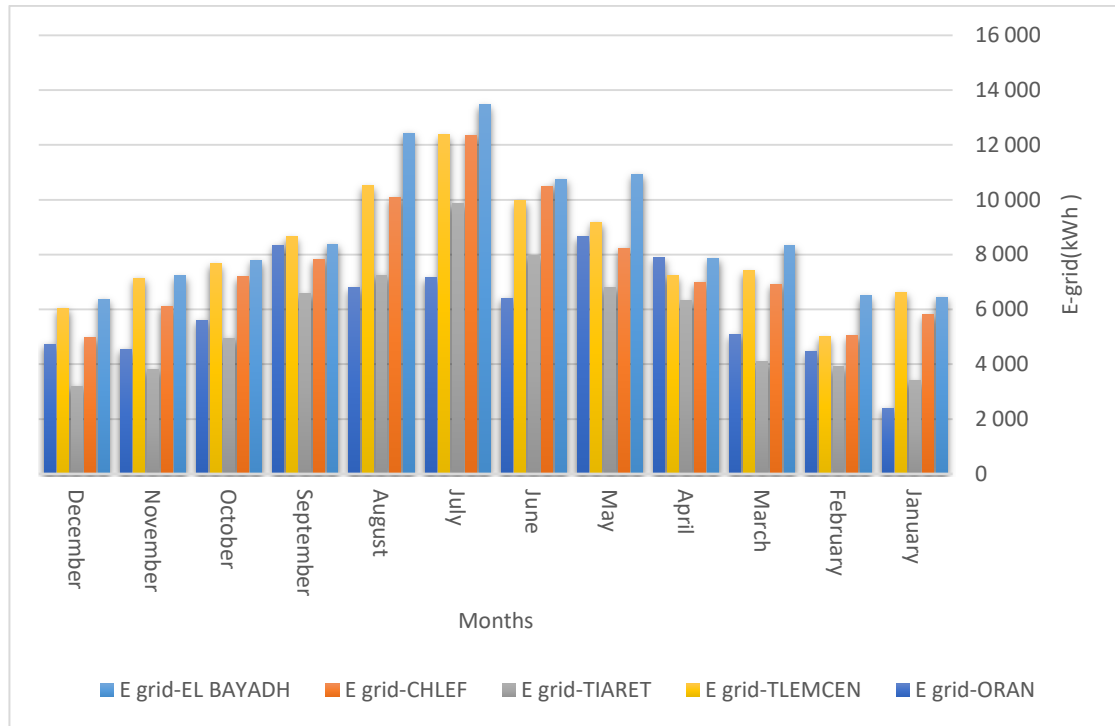


Figure III.7: Dish output of the western states of Algeria

### 5.1.1 Analysis and discussion

Columns graphs represent changes dish output in terms of months, where El-Bayadh the highest recorded value of the production of electrical energy compared to all of Oran and Tlemcen and Tiaret and Chlef estimated at 13456 kWh followed by the state of Tlemcen at 12368 kWh and then the state of Chlef at 12358 kWh followed by Tiaret to 9864 kWh respectively. This in the month of July either Oran province it has recorded the highest production value in the month of May was estimated at 8645 kWh.

### 5.2 Irradiation on dish area (H-sol)

The following table represents the production of irradiation on dish area for 5 solar dishes in the western Algerian states.

	El-Bayadh (kWh)	Chlef (kWh)	Tiaret (kWh)	Tlemcen (kWh)	Oran (kWh)
January	41 183	37 712	26 288	42 009	20 205
February	41 183	34 025	27 230	33 665	31 955
March	51 748	45 659	31 159	48 144	36 660
April	50 990	47 138	42 045	48 483	50 792



May	66 916	54 582	46 660	58 717	58 087
June	67 292	68 149	54 850	65 287	48 363
July	<b>81 056</b>	<b>76 689</b>	<b>65 053</b>	<b>76 065</b>	51 715
August	74 836	64 675	52 413	66 550	49 362
September	52 561	51 297	44 473	55 044	<b>54 065</b>
October	50 695	47 188	35 466	49 102	39 527
November	44 375	39 959	27 510	45 224	31 694
December	40 061	33 195	25 645	37 908	32 606

Table III.14: irradiation on dish area of the western states of Algeria

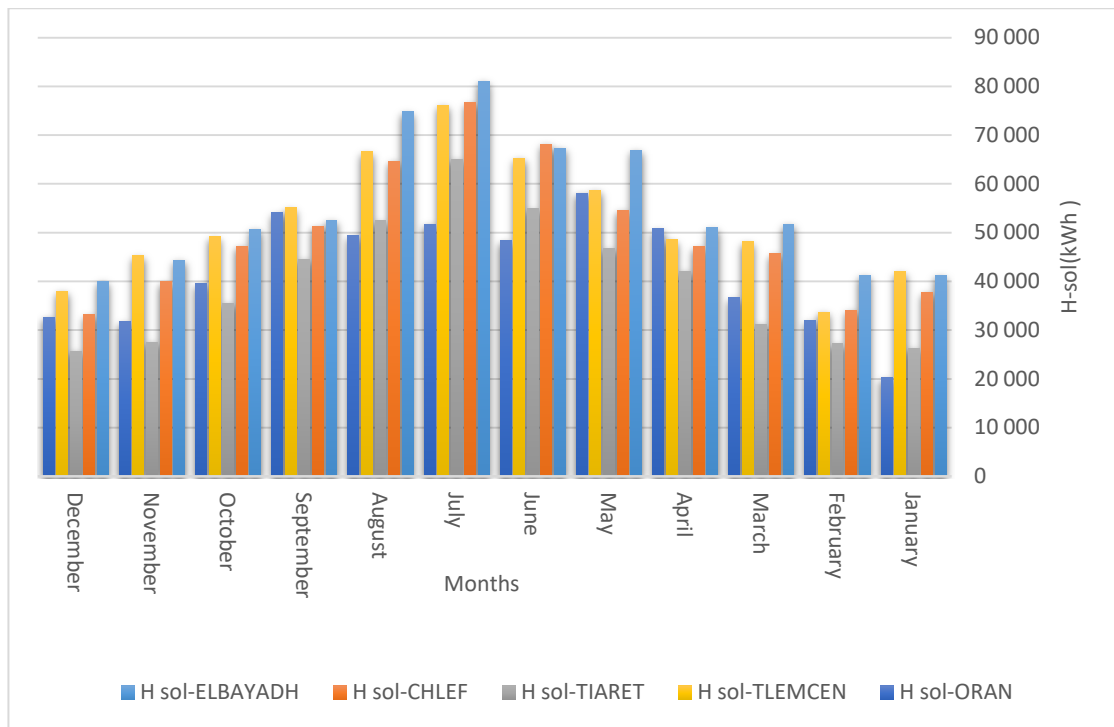


Figure III.8: irradiation on dish area of the western states of Algeria

### 5.2.1 Analysis and discussion

Columns graphs represent changes irradiation on dish area in terms of months, where El-Bayadh the highest recorded value of the production of electrical energy compared to all of Oran and Tlemcen and Tiaret and Chlef estimated at 81056 kWh followed by the state of Chlef at 76689 kWh and then the state of Tlemcen at 76065 kWh followed by Tiaret to 65053 kWh respectively. This in the month of July either Oran province it has recorded the highest production value in the month of May was estimated at 58087 kWh.

### Chapter III: Simulation by software GREENIUS

The following table represents the technical results of electric power plant using 5 dishes in the western Algerian states.

Technical Key Results	El-Bayadh	Chlef	Tiaret	Tlemcen	Oran
Meteorological Data :					
<b>Global horizontal irradiance (GHI)</b>	<b>1955.47</b>	<b>1884.53</b>	<b>1714.55</b>	<b>1934.57</b>	<b>1793.33kWh/ (m<sup>2</sup>·a)</b>
<b>Direct normal irradiance (DNI)</b>	<b>2338.26</b>	<b>2117.34</b>	<b>1688.86</b>	<b>2208.81</b>	<b>1781.41kWh/ (m<sup>2</sup>·a)</b>
Diffuse horizontal irradiance (Diff)	562.06	607.96	689.09	607.82	712.59kWh/ (m <sup>2</sup> ·a)
Mean Annual ambient temperature	15.72	18.08	18.61	17.80	18.23°C
Site Position and Orientation :					
Site	Default	Default	Default	Default	Default
Latitude	33.67	36.22	35.25	35.02	35.68°N
Longitude	1.00	1.33	1.43	-1.47	-0.60°E
Dish/Stirling System Characteristics :					
Installed capacity	0.05	0.05	0.05	0.05	0.05 MW
Number of units	5	5	5	5	5
Capacity per System	10.00	10.00	10.00	10.00	10.00 kW
Simulation Results:					
Total annual net elect. output	106.46	92.02	68.09	97.76	72.09MWh
Total annual gross elect. output	115.04	100.51	75.47	106.43	79.63MWh
Mean system efficiency	16.06	15.33	14.22	15.61	14.27 %

Table III.15: Technical Key Results of the western states of Algeria

The following table represents the economic results of electric power plant using 5 dishes in the western Algerian states

Economic Key Results	El-Bayadh	Chlef	Tiaret	Tlemcen	Oran
Financial Input Parameters :					
Electricity Tariff	0.1700	0.1700	0.1700	0.1700	0.1700€/kWh

### Chapter III: Simulation by software GREENIUS

Grant Proportion (Renewable)	0.00	0.00	0.00	0.00	0.00 %
Debt-Equity-Ratio	70.00	70.00	70.00	70.00	70.00 %
Average Interest Rate	5.64	5.64	5.64	5.64	5.64 %
Simulation Results :					
Internal Rate of Return (IRR) on Equity	-14.26	-16.03	-20.39	-15.28	-19.44%
Net Present Value	-661,620	-682,356	-716,684	-674,118	-710,952€
Payback Period	0.00	0.00	0.00	0.00	0.00 yrs.
Discounted Payback Period	0.00	0.00	0.00	0.00	0.00 yrs.
Total Incremental Costs	810,339	819,574	834,864	815,905	832,311€
Minimum ADSCR	0.06	0.02	-0.12	0.04	-0.10
Required Tariff (LCOE)	1.2186	1.4100	1.9053	1.3271	1.7998 €/kWh
Incremental LEC	0.5954	0.6968	0.9591	0.6529	0.9032€/kWh
Calculation of LEC					
<b>Levelized Electricity Costs (LEC)</b>	<b>0.6454</b>	<b>0.7468</b>	<b>1.0091</b>	<b>0.7029</b>	<b>0.9532€/kWh</b>
<b>Total Investment Costs (IC)</b>	<b>782,512</b>	<b>782,512</b>	<b>782,512</b>	<b>782,512</b>	<b>782,512€</b>
Annuity of IC	0.08	0.08	0.08	0.08	0.08
NPV of Running Costs (OC)	95,875	95,875	95,875	95,875	95,875€
Annuity of OC	0.08	0.08	0.08	0.08	0.08
Environmental Aspects :					
<b>Annual CO2 Reduction</b>	<b>63.88</b>	<b>55.21</b>	<b>40.86</b>	<b>58.65</b>	<b>43.25t CO2</b>

Table III.16: Economic key results of the western states of Algeria

### **5.3 Interpretation**

The priority of the state of El-Bayadh over the rest of the western states in terms of the results of dish output and irradiation on dish area to have a higher global horizontal irradiation and direct normal irradiance, this is from the technical side, but from the economic side, El-Bayadh state has the lowest cost recovery period for the establishment and manufacture.

## **6 Summary of the third chapter**

through studies and the use of software simulation GREENIUS we reached that the greater global horizontal irradiation has increased the productivity of the solar dish and these circumstances solar dishes operate under the temperature of an optimal 15°C give the highest efficiency of her and therefore the intensity of solar radiation and temperature factors influencing the dishes productivity of solar.

**Chapter IV:  
Simulation by  
software System  
Advisor Model  
and an applied  
simulation**

## 1. An introduction

In this chapter, we will discuss the study of the electrical energy productivity of dish stirling systems for some states of the east, west, north and south of Algeria, through the use of simulation programs SAM and comparing the results.

## 2. Simulation by software SAM

### 2.1 The northern states

The following table represents the production of electrical energy for 5 solar dishes in the some northern Algerian states.

	Monthly Energy   (kWh)-Alger	Monthly Energy   (kWh)-Annaba	Monthly Energy   (kWh)-Bejaïa	Monthly Energy   (kWh)-Jijel	Monthly Energy   (kWh)-Skikda
January	5759,94	8657,58	10575,3	8070	9106,42
February	8471,2	7568,27	8819,73	9285,57	7627,77
March	10160,8	11702,3	11832,7	9739,64	11801,9
April	12491	10853	11836,3	13506,7	12154
May	14361,8	14570,4	13498,2	15307,4	16110,5
June	15798	17634,3	17928	18428,1	19847,4
July	<b>19480</b>	<b>19805,8</b>	<b>20290</b>	<b>22071,8</b>	<b>23788,2</b>
August	14905,7	17352,2	16325,1	16532,3	16300,9
September	12957,2	15179,9	13020,8	15243,6	13308,7
October	9306,45	13636,6	10143	11907,2	11630,8
November	7123,83	10668,5	11161,8	9098,01	8432,52
December	7559,66	9505,13	9080,7	7703,06	9378,3

Table IV.1: Monthly energy of the northern states of Algeria

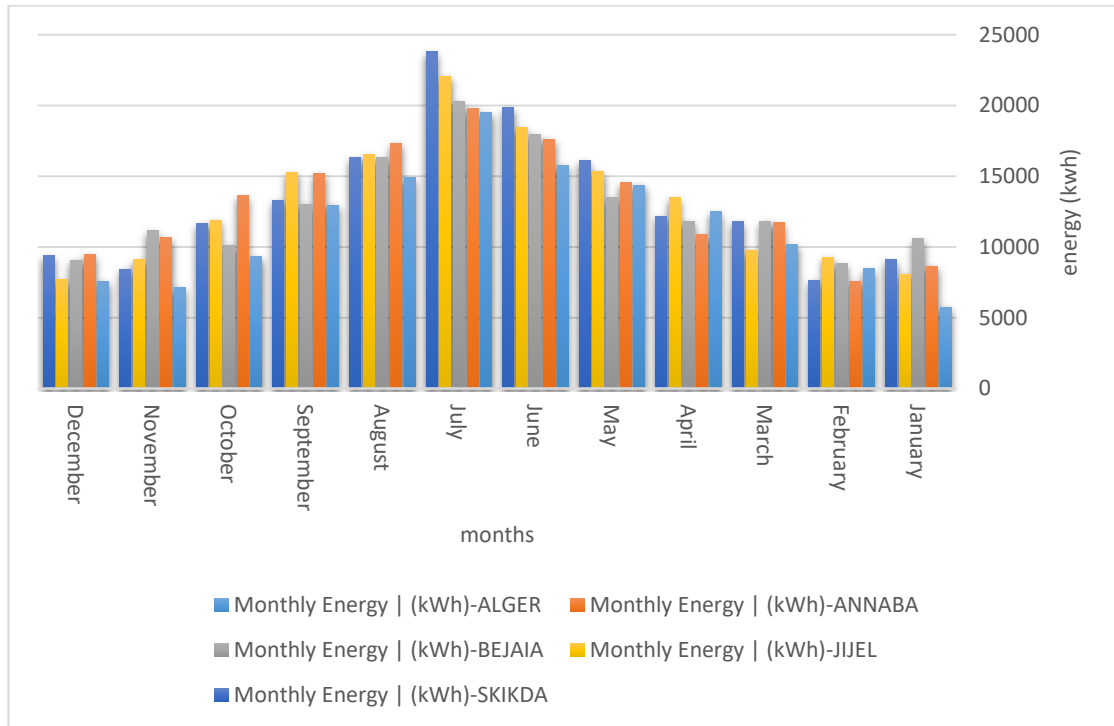


Figure IV.1: Monthly energy of the northern states of Algeria

### 2.1.1 Analysis and discussion

The columns represent the changes of monthly energy of the northern states of Algerian terms of the months of the northern states of Algeria, where we note that the best northern state is the state of Skikda compared to other states, where it reached its maximum value estimated at 23788 kWh followed directly by the state of Jijel and estimated at 22071.8 kWh, followed by each of Bejaia with 20290 kWh, then Annaba with 19805.8 kWh and Algeria with 19480 kWh on the order and this is during the month of July.

### 2.1.2 Interpretation

Skikda is the best of terms of electric energy production compared to other states because it has the highest solar radiation.

## 2.2 The eastern states

The following table represents the production of electrical energy for 5 solar dishes in the some eastern Algerian states.

	Monthly Energy   (kWh)-Biskra	Monthly Energy   (kWh)-Bordj Bou Arreridj	Monthly Energy   (kWh)-Constantine	Monthly Energy   (kWh)-Guelma	Monthly Energy   (kWh)-Batna
January	9633,28	8577,81	6208,51	2975,98	8378,38
February	7692,03	7509,76	6980,79	3318,98	7543,52
March	11328,8	10903,2	8843,75	2998,31	10368,6
April	9633,79	10006,2	9305,06	3565,86	9290,17
May	9766,44	12514,8	10817,5	3465,64	11723,2
June	10514,8	13814,8	13344,2	2621,8	13181,8
July	<b>12790</b>	<b>16528,8</b>	<b>16533,2</b>	3519,42	<b>16395,9</b>
August	10322,7	14251,9	12856,3	4130,64	13350,6
September	8109,32	10321,3	10300,1	<b>4277,76</b>	11331,2
October	7504,09	10470,6	8415,71	4017,06	9961,82
November	9937,83	8476,92	7146,76	3765,64	9627,5
December	8798,94	8700,25	7158,22	4113,1	8200,71

Table IV.2: Monthly energy of the eastern states of Algeria

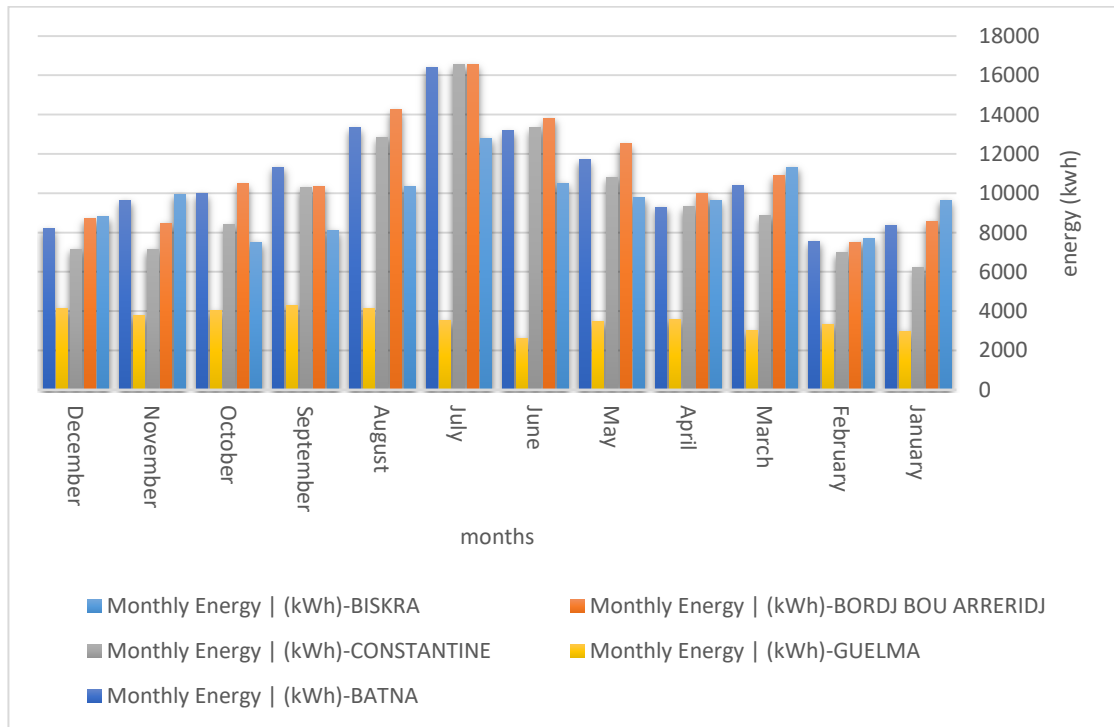


Figure IV.2: Monthly energy of the eastern states of Algeria



### 2.2.1 Analysis and discussion

Columns graphs represent changes monthly energy of the eastern states of Algeria in terms of months, where Constantine the highest recorded value of the production of electrical energy compared to all of Guelma and Biskra and Constantine and Bordj Bou Arreridj estimated at 16533.2 kWh followed by the state of Bordj Bou Arreridj at 16528.8 kWh and then the state of Batna at 16395.9 kWh followed by Biskra to 12790 kWh respectively. This in the month of July either Guelma province it has recorded the highest production value in the month of September was estimated at 4277.76 kWh.

### 2.2.2 Interpretation

Constantine is the best of terms of electric energy production compared to other states because it has the highest solar radiation.

### 2.3. The southern states of Algeria

The following table represents the production of electrical energy for 5 solar dishes in the some southern Algerian states.

	Monthly Energy   (kWh)-Adrar	Monthly Energy   (kWh)-Ghardaïa	Monthly Energy   (kWh)-In Saleh	Monthly Energy   (kWh)-Ouargla	Monthly Energy   (kWh)-Tamanrasset
January	<b>15063,30</b>	13931,80	<b>14772,50</b>	6705,08	<b>16150,40</b>
February	11619,10	12385,90	9851,69	5467,09	15618,90
March	13983,50	<b>15378,90</b>	12167,50	5651,14	15558,40
April	12462,40	13813,10	10270,90	5126,43	13013,40
May	11417,90	13693,70	10195,80	6461,25	10972,70
June	11828,70	14342,10	10248,20	5535,01	12791,70
July	11562,60	15187,20	10868,00	5500,35	12302,70
August	11595,40	12992,30	11223,20	6117,79	10725,60
September	10227,00	11835,90	9719,30	6311,32	9479,77
October	10541,20	11679,30	9886,82	7175,38	12977,40
November	13046,00	13295,80	11961,60	6852,97	11511,40
December	14205,30	12560,40	12694,60	<b>7261,31</b>	12501,50

Table IV.3: Monthly energy of the southern states of Algeria

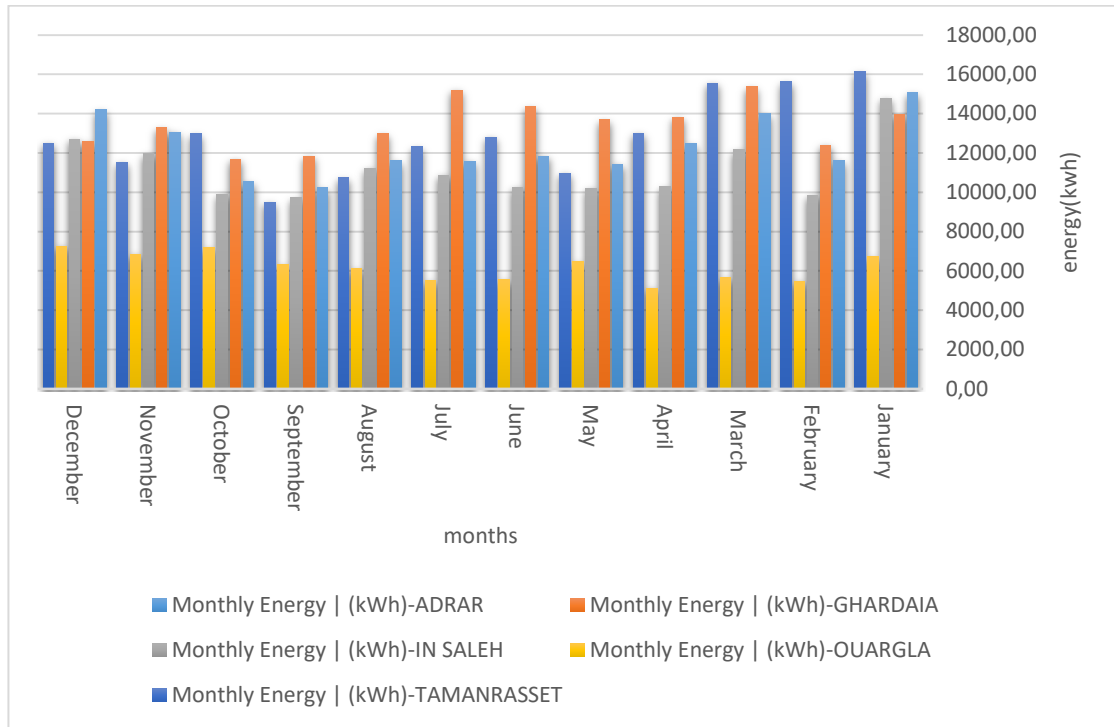


Figure IV.3: Monthly energy of the southern states of Algeria

### 2.3.1 Analysis and discussion

Columns graphs represent changes monthly energy of the southern states in terms of months, where Tamanrasset recorded the highest value of electrical energy production compared to all of Ouargla and Adrar and Ghardaïa estimated at 16150.4 kWh in January, followed by the state of Ghardaïa with 15378.9 kWh in March and then the state of Adrar with 15063.3 kWh in January, followed by In-Saleh with 14772.56 kWh in January, followed by state of Ouargla with 7261.31 kWh in December.

### 2.3.2 Interpretation

Tamanrasset is the best of terms of electric energy production compared to other states because it has the highest solar radiation.

## 2.4 The western states of Algeria

The following table represents the production of electrical energy for 5 solar dishes in the some western Algerian states.

	Monthly Energy   (kWh)-El-Bayadh	Monthly Energy   (kWh)-Chlef	Monthly Energy   (kWh)-Tiaret	Monthly Energy   (kWh)-Tlemcen	Monthly Energy   (kWh)-Oran
January	829,183	7348,44	7177,62	8698,41	2793,33
February	646,718	6362,65	6641,23	6697,32	5019,21
March	813,949	8371,04	9583,72	9802,98	5934,93
April	604,499	8334,90	9691,82	8655,59	8242,47
May	945,601	9592,33	9811,38	11245	8892,41
June	961,744	12167,60	14077,60	12259,7	6769
July	<b>1019,27</b>	<b>14570,60</b>	<b>15702,00</b>	<b>14905</b>	7154,37
August	1094,4	11970,20	14724,80	12884,4	7309,9
September	818,789	9479,30	11299,70	10618,2	<b>9422,55</b>
October	726,247	8966,25	10053,10	10054,3	6593,61
November	778,424	7934,21	8016,12	9453,96	5444,96
December	603,356	6101,40	5664,52	7719,47	5513,99

Table IV.4: Monthly energy of the western states of Algeria

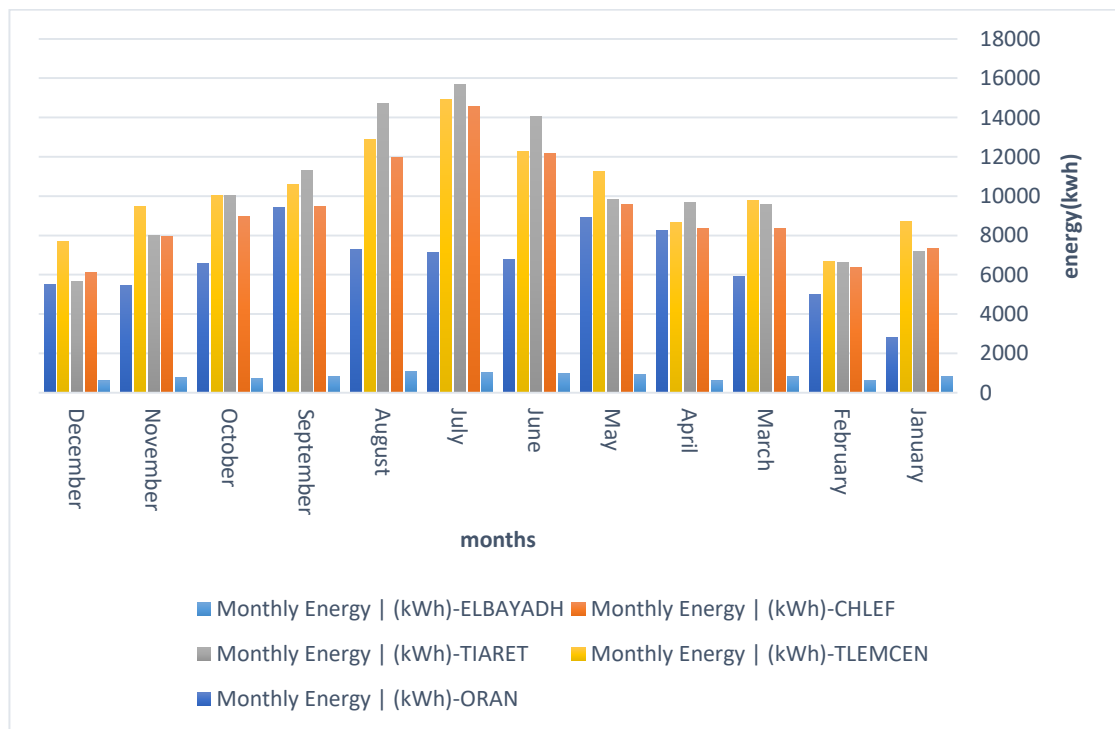


Figure IV.4: Monthly energy of the western states of Algeria

### **2.4.1 Analysis and discussion**

Columns graphs represent changes monthly energy of the western states of Algeria in terms of months, where Tiaret the highest recorded value of the production of electrical energy compared to all of Chlef and Tlemcen and Oran and El-Bayadh estimated at 15702 kWh followed by the state of Tlemcen at 14905 kWh and then the state of Chlef at 145706 kWh respectively. This in the month of July either Oran province it has recorded the highest production value in the month of September was estimated at 9422.55 kWh followed by the state of El-Bayadh at 1094.4 kWh in August.

### **2.4.2 Interpretation**

Tiaret is the best of terms of electric energy production compared to other states because it has the highest solar radiation.

## **3. An applied simulation**

For the purpose of studying the performance of solar dishes and knowing how to produce electrical energy. The preparations of a small project is the solar dish and make some experiments to determine the temperature and the intensity of solar radiation as well as the effect of wind speed on the performance of the solar dish using this measurement tools:



Figure IV.5: Mini solar dish project

Some results for the solar dish were obtained using the following measurement tools:



Figure IV.6: Thermometer solar model  
OMEGA RDXL4SD



Figure IV.7: Thermal pickup



Figure IV.8: Mini anemometers model  
UT363



Figure IV.9: Solar Power Meter

## Chapter IV: Simulation by software System Advisor Model and An Applied simulation

Time	12:25	12:35	12:40	12:50	13:00	13:05	13:10	13:15	13:20
Temperature(°C)	255.9	260	280	222	244	240	286	281	284
Irradiation(W/m <sup>2</sup> )	1036	1070	1108	1050	1056	1005	1094	1086	1077
Wind speed(m/s)	0.6	0.5	0	1	0.3	0.3	0.2	0.2	0.2

Table IV.5: An applied simulation

time	temperature (°C)
12:25	255,9
12:35	260
12:40	280
12:50	222
13:00	244
13:05	240
13:10	286
13:15	281
13:20	284

Table IV.6: Temperature in terms of time

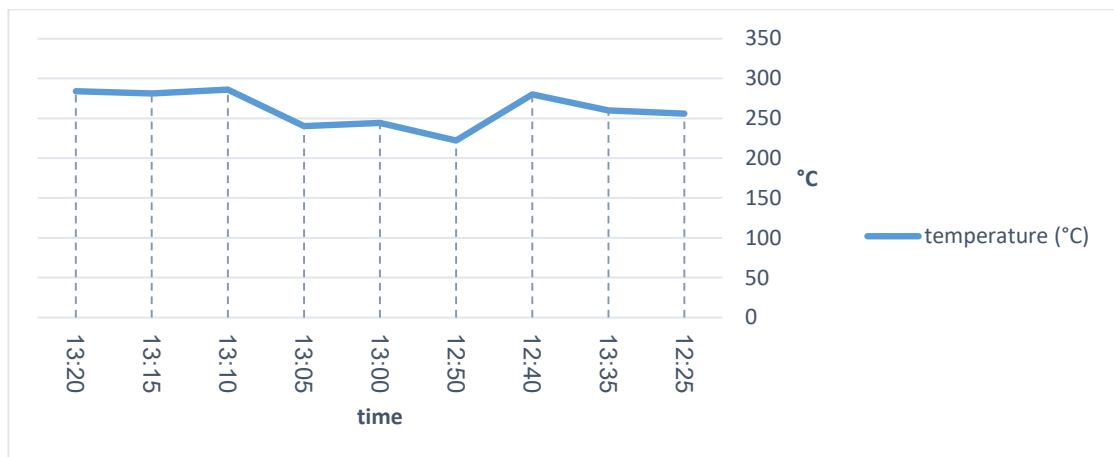


Figure IV.10: Temperature in terms of time

Time	Irradiation(W/m <sup>2</sup> )
12:25	1036
12:35	1070
12:40	1108

12:50	1050
13:00	1056
13:05	1005
13:10	1094
13:15	1086
13:20	1077

Table IV.7: irradiation in terms of time

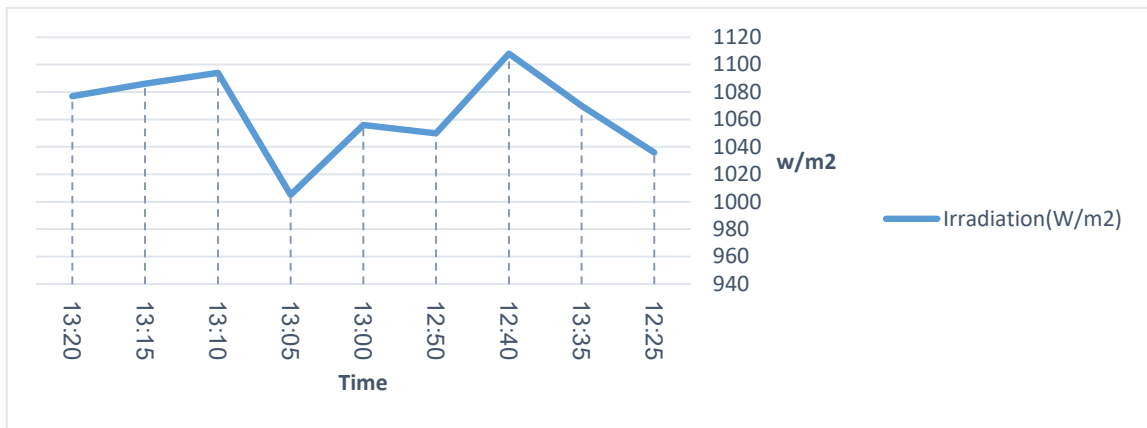


Figure IV.11: irradiation in terms of time

time	wind speed (m/s)
12:25	0,6
12:35	0,5
12:40	0
12:50	1
13:00	0,3
13:05	0,3
13:10	0,2
13:15	0,2
13:20	0,2

Table IV.8: Wind speed in terms of time



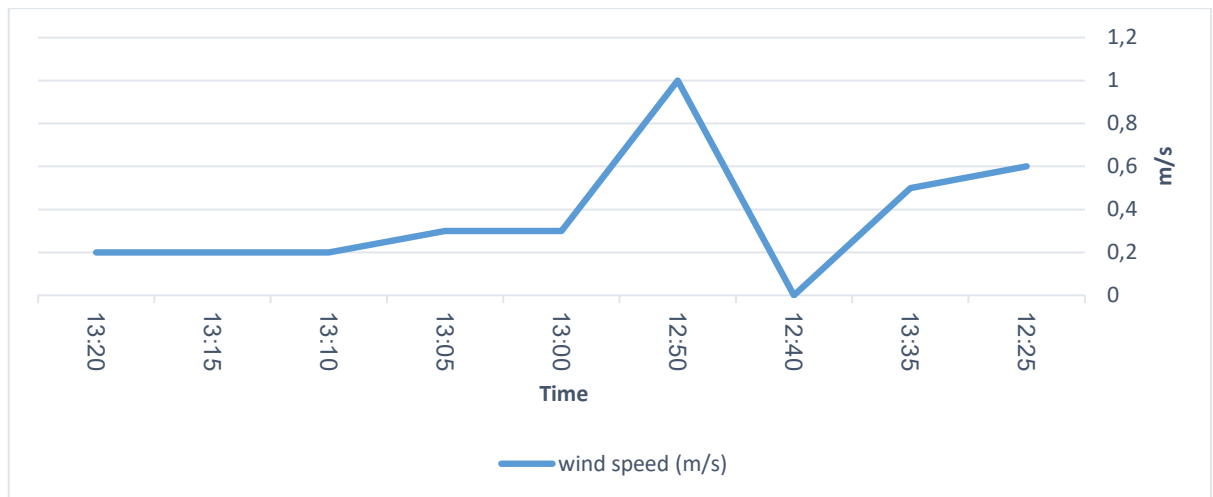


Figure IV.12: Wind speed in terms of time

### 3.1 Analysis and interpretation

The curves represent changes in temperature, solar radiation intensity, and wind speed in terms of time. We notice fluctuations in results over time.

The increase in the production of electric power back solar dishes to the high intensity of heat generated through solar dishes due to the high intensity of solar radiation and low wind speed.

## 4. Ideal Stirling Cycle Calculator

### 4.1. Calculator Inputs:

The table represents the calculator's input for the measured values of temperature, pressure, volume, and specific heat  $C_p$  for hydrogen at (20 C° and  $P_{atm}=1.013Pa$ ), for the city of Ouargla.

Hot end temperature (K):	430.1
Cold end temperature (K):	309
Compression Ratio:	2
Specific gas constant of working fluid (J/kg-K):	14240
Pressure at state 1 (kPa):	103
Volume at state 1 (cc):	45
Amount of heat applied to engine (W):	3500

Table IV.9.calculator inputs related to the sterling engine [21].

## 4.2. Calculator Outputs:

The table represents the calculator's outputs.

Calculation Status: Inputs OK	
Predicted Frequency (RPM)	4.696e+4
Predicted Power Out (W)	985.5
Predicted Efficiency (0-1)	0.2816
Predicted Average Pressure (kPa)	177.8
Swept Volume (cc)	22.50
Mass of Working Fluid (mg)	1.053
Work Out Per Cycle (J)	1.259
Predicted Specific Work Out Per Cycle (J/mg-working fluid)	1.195
Volume at State 1 (cc)	45.00
Absolute Pressure at State 1 (kPa)	103.0
Temperature at State 1 (K)	309.0
Volume at State 2 (cc)	22.50
Absolute Pressure at State 2 (kPa)	206.0
Temperature at State 2 (K)	309.0
Volume at State 3 (cc)	22.50
Absolute Pressure at State 3 (kPa)	286.7
Temperature at State 3 (K)	430.1
Volume at State 4 (cc)	45.00
Absolute Pressure at State 4 (kPa)	143.4
Temperature at State 4 (K)	430.1

Table IV.10.calculator output related to the sterling engine [21].

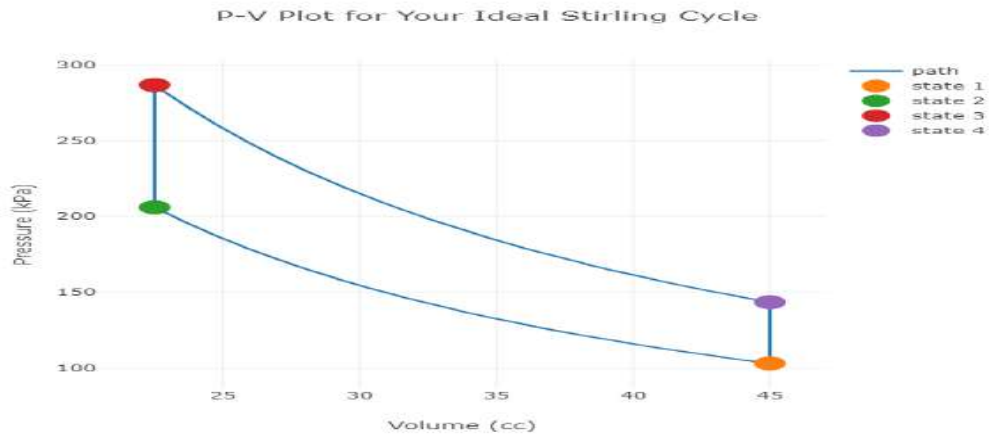


Figure IV.13. P-V diagram of the ideal stirling cycle[21].

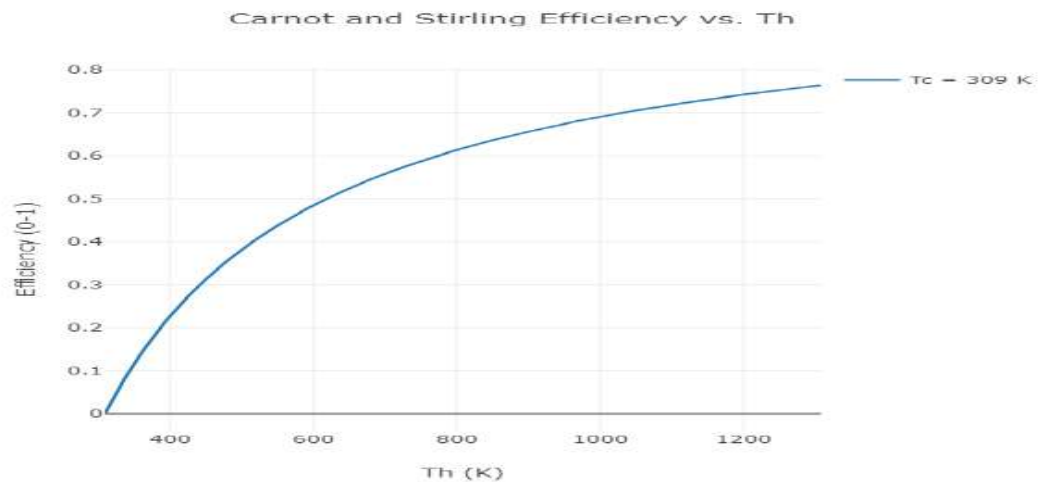


Figure IV.14. Carnot and stirling efficiency diagram[21].

### 4.3. Analysis and interpretation :

The diagram (IV.13) represents the pressure changes in terms of volume, for the ideal Stirling cycle, Where we notice a gradual increase from state 1 to state 2, then a sharp increase from state 2 to state 3, gradually decreasing from state 3 to state 4, finally There is a sharp decrease from case 4 to case 1.

Graph (IV.14) represents the changes in efficiency in terms of temperature, for Carnot and Stirling efficiency, where we see that the higher the temperature  $T_h$ , the higher the efficiency.

The diagram (IV.13) where two transformations occur under constant temperature from state 1 to state 2, and from state 3 to state 4, and two transformations under constant volume, from state 2 to state 3, and from state 4 to state 1.

In graph (IV.14), the reason for the increase in efficiency with an increase in temperature is the difference in temperature between the inside and outside of the Stirling engine, and from it the more difference in temperature increase the efficiency of the stirling engine and vice versa.

### **5. Summary of the Forth**

In this chapter, we have studied the simulation of the production of solar dishes in the states of the east, west, north and south of Algeria through the use of the simulation software SAM we have found that the northern, western, and eastern states up the highest production in the month of July on. As for the southern states, they reach their highest production in the winter, but in the summer, and in July, temperature is very high, which negatively affects the efficiency of the solar dishes.

# **General Conclusion**

# General Conclusion

Energy is one of the most important pillars of life, especially in human life, because it provides various uses in various fields of life, and this is what made him think of ways and means to extract and make better use of energy. Due to the discovery of fossil energies as a primary energy source and excessive dependence on it, which resulted in many negatives from the environmental side, the attention of thinkers and scientists turned towards an energy source that would be safer and more available, among them renewable energies, which are the focus of attention, including concentrating solar thermal systems or what is known in solar dishes, it is one of the most important solar thermal concentration systems in terms of production performance, which works to focus the incoming sunlight in one point at the level of the future by means of reflective mirrors.

Through our study of 5 solar dishes, we have reached important theoretical results among them:

- Skikda state is the best northern state in terms of electricity production, with an estimated value of 23788.2 kWh in July.
- Constantine state is the best eastern state in terms of electricity production, with an estimated value of 16533.2 kWh in July.
- Ghardaïa state is the best southern state in terms of electricity production, with an estimated value of 16150.4 kWh in January.
- Tiaret state is the best western state in terms of electricity production, with an estimated value of 15702 kWh in July.

After the experimental study, it became clear to us that the higher difference in temperature between inside and outside of Stirling engine and the intensity of solar radiation, the more efficient the solar dish and vice versa, as we have reached some results, including :

- Higher global horizontal irradiation estimated at  $1108 \text{ w/m}^2$  at 12:40 PM.
- Higher concentrated temperature was estimated at  $286^\circ\text{C}$  at 13:10 PM.
- Predicted power out of dish Stirling in state of Ouargla at a temperature ( $T_{\text{heat}}=430.1\text{K}$ ,  $T_{\text{cold}}=309\text{K}$ ) estimated at 985.5 watts.
- Climatic factors have a negative impact on the efficiency of the solar dish.

## Most important recommendations

We mention the most important recommendations and solution for the future studies and projects:

1. Increase in the reflective area of the solar dish.
2. Finding more reflective substance.
3. The fluid is highly conductive and has a heat storage capacity.

# **Bibliographic references**



## Bibliographic References

- [1] International Energy Agency, “World Energy Outlook 2016,” pp. 1–684, 2016.
- [2] GarridoGálvez J. *Solar cavity receiver design for a dish-Stirling system* (Doctoral dissertation, KTH Royal Institute of Technology).
- [3] Lanini F. Division of global radiation into direct radiation and diffuse radiation. University of Bern. 2010.
- [4] Bjelopavlić, D.; Todorović, M.: Solarnipaneli, 2010. (<http://solarnipaneli.org/>).
- [5] Serifi, V.; Sofiu, V. An overview of direct solar irradiation. Sokobanja. Serbia. 2011. (<https://www.researchgate.net/publication/338633301>).
- [6] Goswami. Kreith and Kreider. Taylor. Francis. Principles of Solar Engineering. Sustainable Energy Science and Engineering Center. 2000. (<http://www.physicalgeography.net>).
- [7] GarridoGálvez J. *Solar cavity receiver design for a dish-Stirling system* (Doctoral dissertation, KTH Royal Institute of Technology).
- [8] International Energy Agency, “World Energy Outlook 2016,” pp. 1–684, 2016.
- [9] Zayed ME, Zhao J, Elsheikh AH, Li W, Sadek S, Aboelmaaref MM. A comprehensive review on Dish/Stirling concentrated solar power systems: Design, optical and geometrical analyses, thermal performance assessment, and applications. *Journal of Cleaner Production*. 2021 Feb 10; 283:124664.
- [10] Stojicevic, M. Jeli, Z. Obradovic, M. Obradovic, R. Gabriel and Marinescu, C. Designs of Solar Concentrators. Faculty of Mechanical Engineering. Belgrade, Vol.47, pp.274-275, 2019.
- [11] Price, H., Lupfert, E., Kearney, D., Zarza, E., Cohen, G., Gee, R. and Mahoney, R.: Advances in parabolic trough solar power technology, *Journal of solar energy engineering*, Vol. 124, No. 2, pp. 109-125, 2002.
- [12] Kumar, A., Prakash, O. and Kaviti, A.K.: A comprehensive review of Scheffler solar collector, *Renewable and Sustainable Energy Reviews*, Vol. 77, pp. 890-898, 2017.

## Bibliographic References

- [13] Prasad, G.C. et al., (2017.) "Optimization of solar linear Fresnel reflector system with secondary concentrator for uniform flux distribution over absorber tube." *Solar Energy*, 150, pp. 1-12.
- [14] Skouri, S et al., (2013.) "Optical, geometric and thermal study for solar parabolic concentrator efficiency improvement under Tunisia environment: A case study." *Energy conversion and management*, 75, pp. 366-373.
- [15] Barreto G, Canhoto P. Modeling of a Stirling engine with parabolic dish for thermal to electric conversion of solar energy. *Energy Conversion and Management*. 2017 Jan.4 pp. 15; 132:119-35.
- [16] Dersch J, Dieckmann S. Techno-economic evaluation of renewable energy projects using the software Greenius. *Int. J. Therm. Environ. Eng.* 17-18 pp. 2015; 10(1):17-24.
- [17] Dobos A, Neises T, Wagner M. Advances in CSP simulation technology in the System Advisor Model. *Energy Procedia*. 2482-2483 pp. 2014 Jan 1; 49:2482-2489.
- [18] Bataineh K, Taamneh Y. Performance analysis of stand-alone solar dish Stirling system for electricity generation. *International Journal of Heat and Technology*. 498-499 pp. 2017 Sep 1; 35(3):498-508.
- [19] Wallander E. Modeling and Control of Dish-Stirling Solar/Gas Hybrid System. 5-6 pp. 2021; 1-51.
- [20] Buscemi A, Brano VL, Chiaruzzi C, Ciulla G, Kalogeri C. A validated energy model of a solar dish-Stirling system considering the cleanliness of mirrors. *Applied Energy*. 16-30 pp. 2020 Feb 15; 260:114378.
- [21] <https://www.mide.com/ideal-stirling-cycle-calculator>.

## ملخص

تعد الطاقات المتجددة من أهم مصادر الطاقة في الكون والتي تساهم في الحفاظ على البيئة وتلبية حاجيات الانسان من جهة أخرى، من أبرزها طاقة الطبق الشمسي أو ما يعرف بأنظمة التركيز الحراري. بعد الدراسة النظرية والتجريبية وانجاز تجربة ميدانية وتحليل ومناقشة المعطيات والنتائج تبين لنا أن انتاجية وكفاءة الطبق الشمسي تعتمد اساسا على شدة الاشعاع الشمسي الصافي ومساحة الطبق في ظل عوامل مناخية جيدة.

في الأخير يمكننا القول أن أنظمة التركيز الشمسي تعتبر أحسن الأنظمة الطاقوية من حيث الكفاءة والإنتاج الكهربائي.

## Résumé

Les énergies renouvelables sont l'une des sources d'énergie les plus importantes de l'univers, qui contribuent à la préservation de l'environnement et à la satisfaction des besoins humains, notamment l'énergie solaire parabolique thermique ou les systèmes thermiques sont connus.

Après l'étude théorique et expérimentale et la réalisation d'une expérience sur le terrain, l'analyse et la discussion des données et des résultats nous montrent que la productivité de la parabole solaire dépend de l'intensité du rayonnement solaire et de la surface nette de la parabole sous de bons facteurs climatiques.

Au final, on peut dire que les systèmes solaires à concentration sont considérés comme les meilleurs systèmes énergétiques en termes d'efficacité et de production électrique.

## Summary

Renewable energies is one of the most important sources of energy in the universe, which contribute to the preservation of the environment and to meet human needs, most notably the solar energy dish thermal or thermal systems focus is known.

After the theoretical and experimental study and the completion of a field experiment and analysis and discussion of the data and results show us that, the solar dish productivity depends on the intensity of the solar radiation and the net area of the dish under good climatic factors.

In the end, we can say that concentrating solar systems are considered the best energy systems in the terms of efficiency and electrical production.